DESIGN AND COMMISIONING OF A LINEARLY POLARIZED GAMMA RAY BEAM FOR PHOTOFISSION EXPERIMENTS

Jasen Swanson
Idaho State University
April 5, 2012

Outline

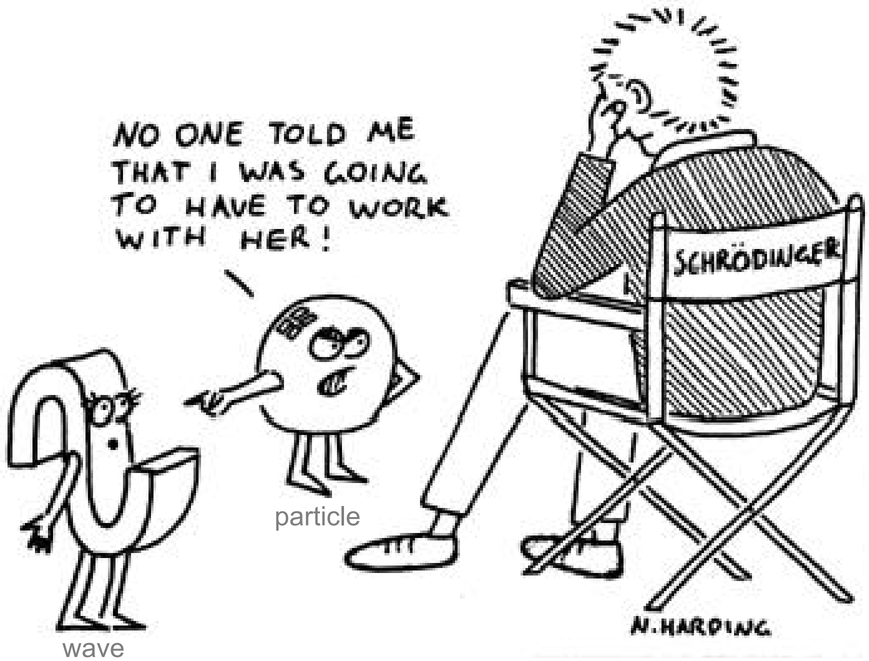

- Motivation
  - Why is this important?
- Theory
  - Photofission
  - History
- Designing a polarized γ–ray beam
  - Photon Production
  - Off-Axis Bremsstrahlung
  - Beam Position Control
  - Photon Flux Monitor
- Polarization Measurements
- Future Work
- Summary

Motivation

- Terror attacks
  - Like September 11
    - Twin Tower-2,753 people died
    - Pentagon-184 people died
    - Shanksville, Pennsylvania-40 people died
- Next might be a nuclear attack
  - Potentially more catastrophic
- Want to prevent such an event

Figure 1: Twin Towers, September 11, 2001

- 3 main ways to smuggle a nuclear weapon
  - Air
  - Land (rail or truck)
  - Water (cargo ship)
- Billions of dollars of commercial goods pass through the ports of the US each month
  - 100's of containers on each ship
  - Nearly impossible to screen every piece of cargo
    - Nuclear weapon could go undetected easily

Figure 2: (Left) Cargo ship transporting hundreds of containers; (Above) Inspectors manually searching through contents of a container for nuclear material.

We want to investigate a technique using linearly polarized photofission to scan the cargo containers for radioactive materials.

Need a polarized photon beam to do that!

What is Photofission?

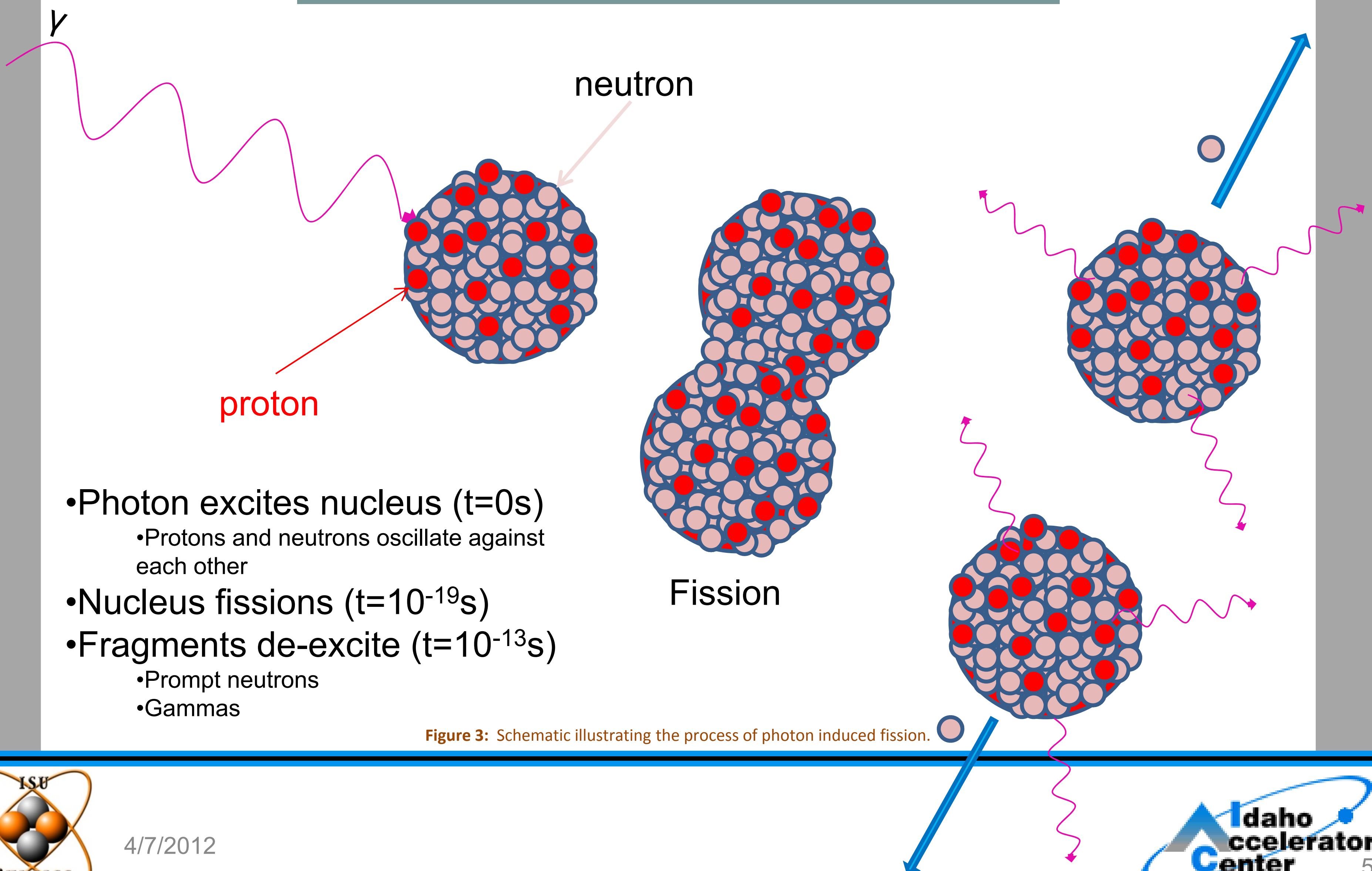

- Photon excites nucleus (t=0s)
  - Protons and neutrons oscillate against each other
- Nucleus fissions (t=10^{-19}s)
- Fragments de-excite (t=10^{-13}s)
  - Prompt neutrons
  - Gammas

Figure 3: Schematic illustrating the process of photon induced fission.

Short History Lesson

- Previous study regarding fission fragment angular distributions [1]
  - 65 MeV Giessen linac
  - Off-axis bremsstrahlung
  - ^{232}Th metallic target (8gm/cm2)
  - Parallel plate avalanche detectors
    - $W(\theta,\phi=0)$ - R_H
    - $W(\theta,\phi=\pi/2)$ -R_V
    - $W(\theta=\pi/2,\phi)$ -R_ϕ

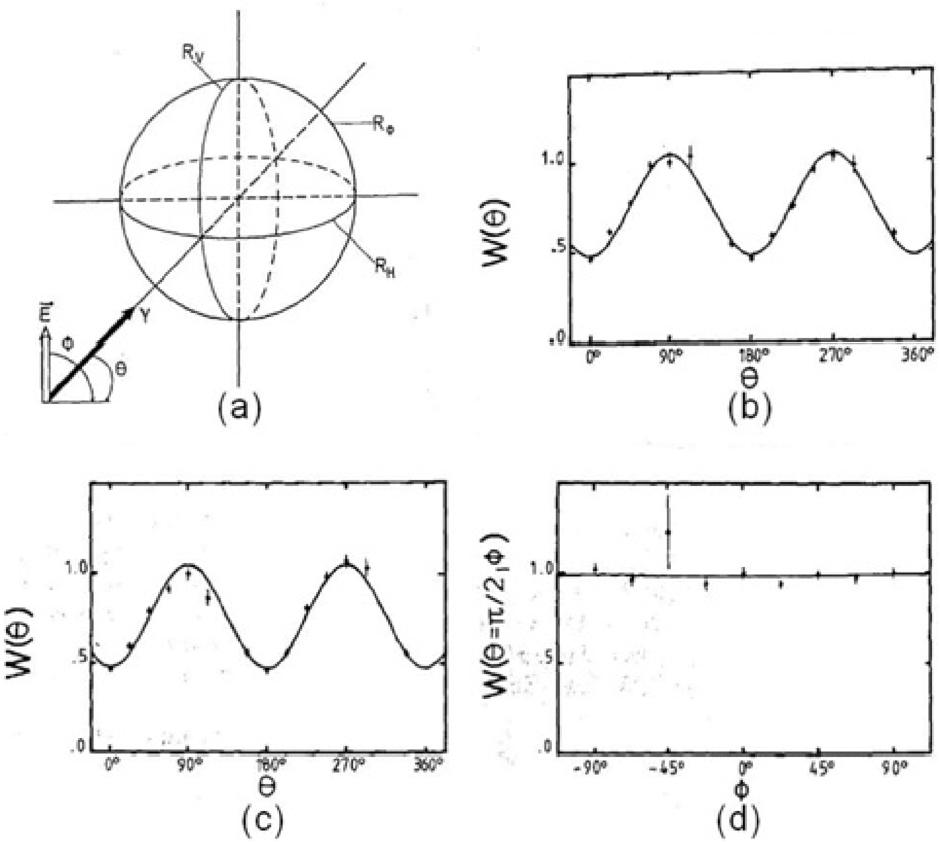

Figure 4: Giessen group experiment on fission fragment angular distributions; (a) experimental setup, and considering unpolarized photons: (b) angular distributions in detector R_H, (c) angular distributions in detector R_V, (d) angular distributions in detector R_φ.

Case 1:Unpolarized Bremsstrahlung

- Considering only E1 transitions of an even-even nucleus
- Identical angular distributions measured by detector rings R_H and R_V
  - Only dependent on polar angle

$$W(\theta) = a + b \sin^2\theta$$

- Fission fragments angular distribution is isotropic in azimuthal angle using unpolarized bremsstrahlung

[1] R. Ratzek et al. Photofission with Polarized Photons, Z. Phys. A.-Atoms and Nuclei. 1982, v. A308, p. 63-71.

History Lesson cont…

- **Case 2: Polarized Bremsstrahlung**
- Considering only E1 transitions of an even-even nucleus
- Two cases of polarization:
  - Electric field vector of the photon is vertical
  - Electric field vector of the photon is horizontal
- Angular distribution depends on both angles θ and Φ:

  $W(\theta, \Phi) = A_0 + A2(P2(\cos\theta) + P\gamma f_2(1,1)\cos 2\Phi\ \ P_2{}^2(\cos\theta))$
    - P_γ is the degree of photon polarization
    - $f_2(1,1) = 3\sin^2\theta$
    - Φ is the azimuthal angle
      - Φ = 0 parallel to **E**
      - Φ = π/2 perpendicular to **E**
- The fission fragments angular distribution in azimuthal angle has a preferred direction corresponding to the electric field vector of the photon

We would like to further explore this, but is well understood that fission fragments are easily stopped in targets as thin as a few mg/cm^2.

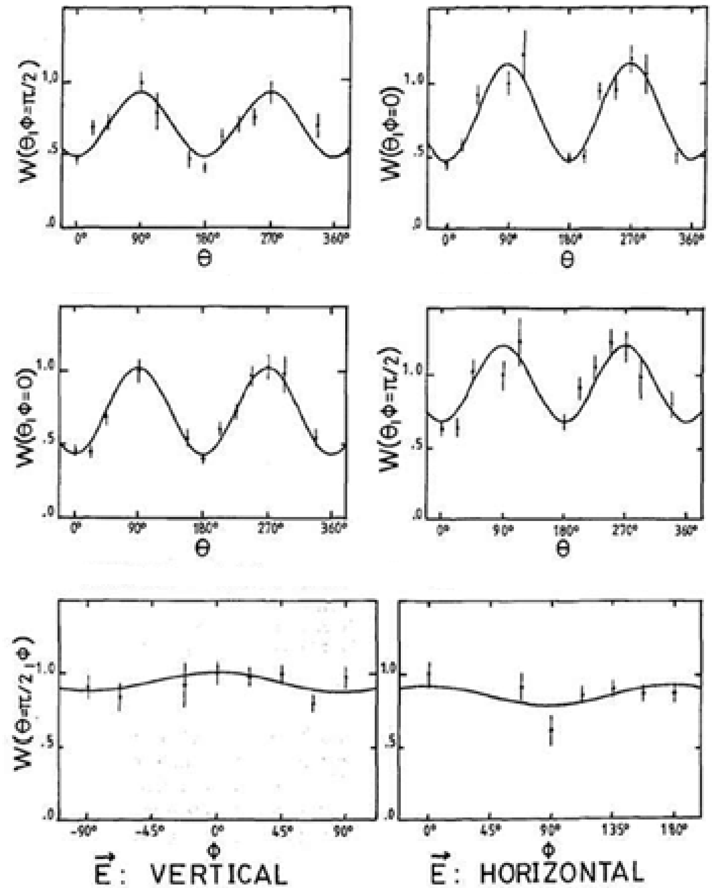

Figure 5: Polarized photon induced fission fragment angular distributions for (left) E-vertical and (right) E-horizontal.

R. Ratzek et al. Photofission with Polarized Photons, Z. Phys. A.-Atoms and Nuclei. 1982, v. A308, p. 63-71.

A Little More History

- 1988, Budtz-Jorgensen and Knitter [2] investigated correlation between the fission fragments and the prompt neutrons which they emit
  - ^{252}Cf
    - Spontaneous fission source
  - Gridded ion chamber
    - Determines fission fragment angle θ, kinetic energy, and mass simultaneously
  - Neutron detector placed outside ion chamber

Concluded that the recoiling fission fragments emit neutrons isotropically in their center of mass

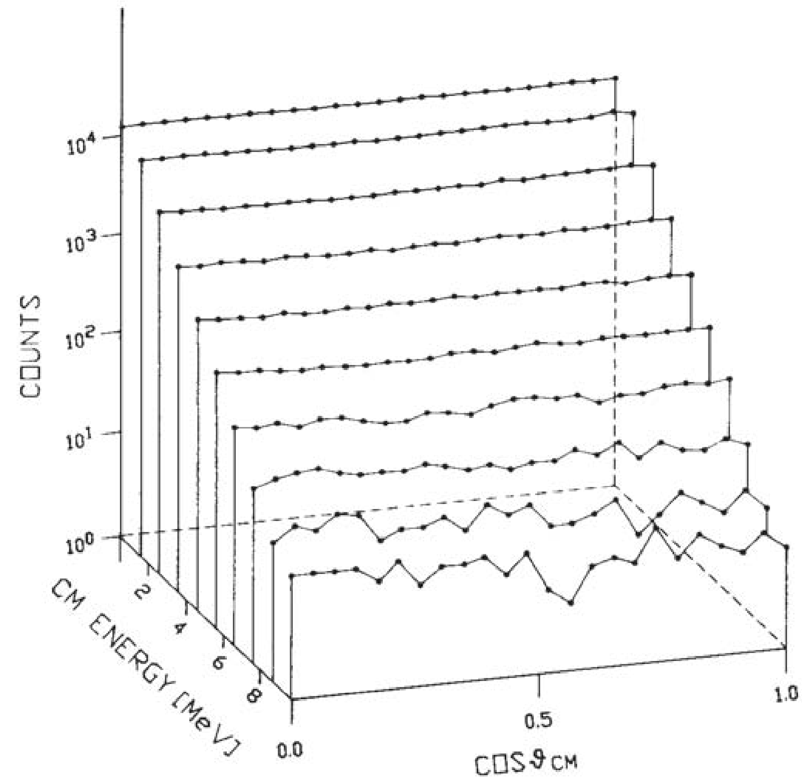

Figure 6: The fission neutron angular distribution as a function of fragment center of mass fission neutron energy .*

C. Budtz-Jorgensen and H.-H. Knitter, Nuc. Phys. A490, 307 (1988)

History Summary

We learned that:

1. Fission fragments recoil in a preferred direction corresponding to the electric field vector of the photon, but fission fragments are easily shielded
2. Recoiling fission fragments emit prompt neutrons isotropically in their center of mass, and those neutrons are not as easily shielded

Thus,

The prompt neutron should travel in a preferred direction corresponding to the electric field vector of the incident photon

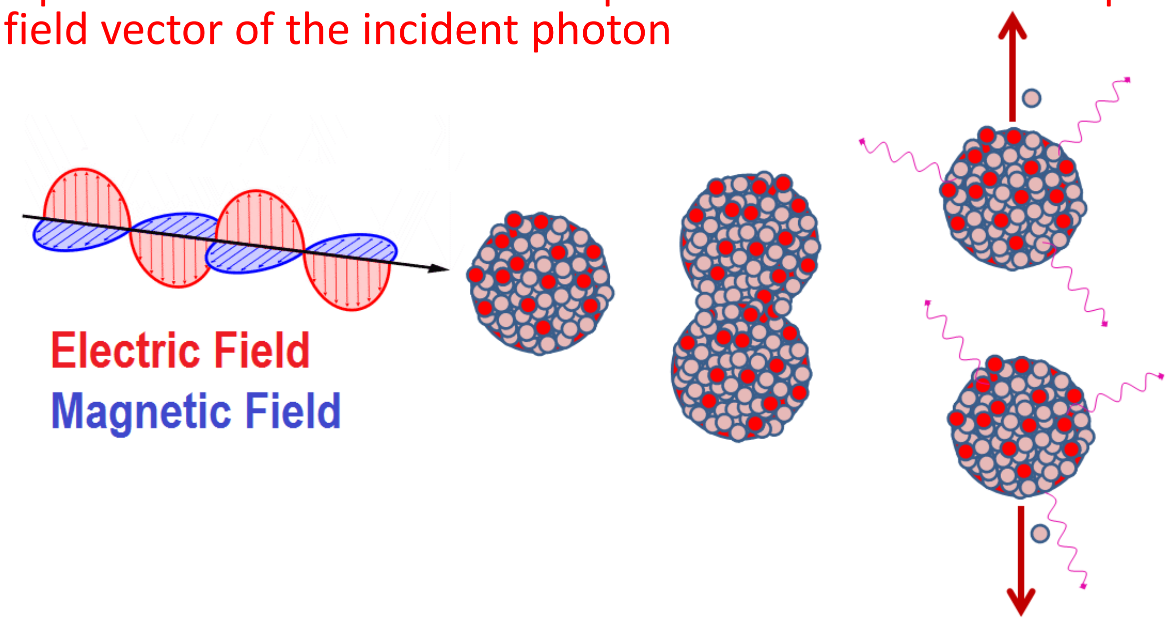

How can we study this using IAC's electron accelerators?

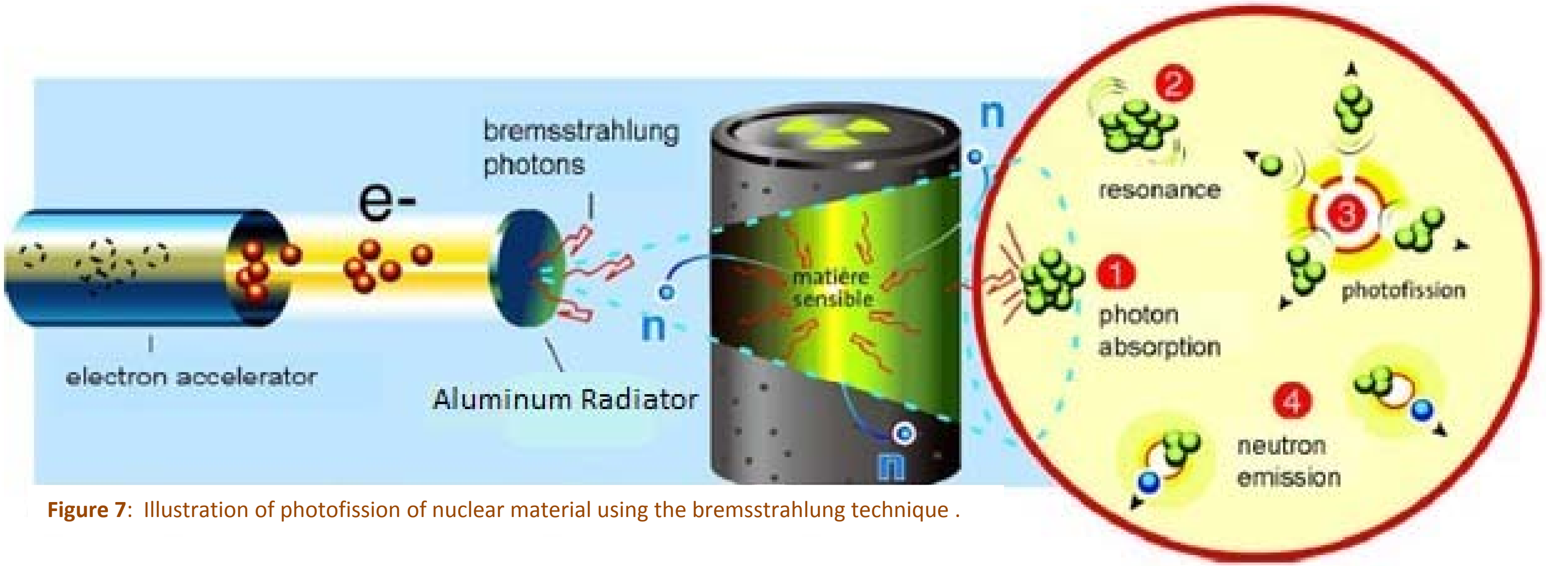

Figure 7: Illustration of photofission of nuclear material using the bremsstrahlung technique .

- Expand upon this well established technique
  - Off-axis bremsstrahlung to induce reactions
    - Know is partially linearly polarized
  - Use knowledge gained from history lesson
    - Measure angular asymmetries of prompt neutrons via polarized photofission of actinides

Photon Production

- Idaho Accelerator Center
- 44-MeV Short Pulsed Linac
  - 1.3 GHz L-band traveling-wave linac
- Beam parameters
  - 25 MeV electron beam energy
  - 500 mA peak current
  - 150 Hz rep rate
  - 2 ns pulse width
  - 1 nC/pulse

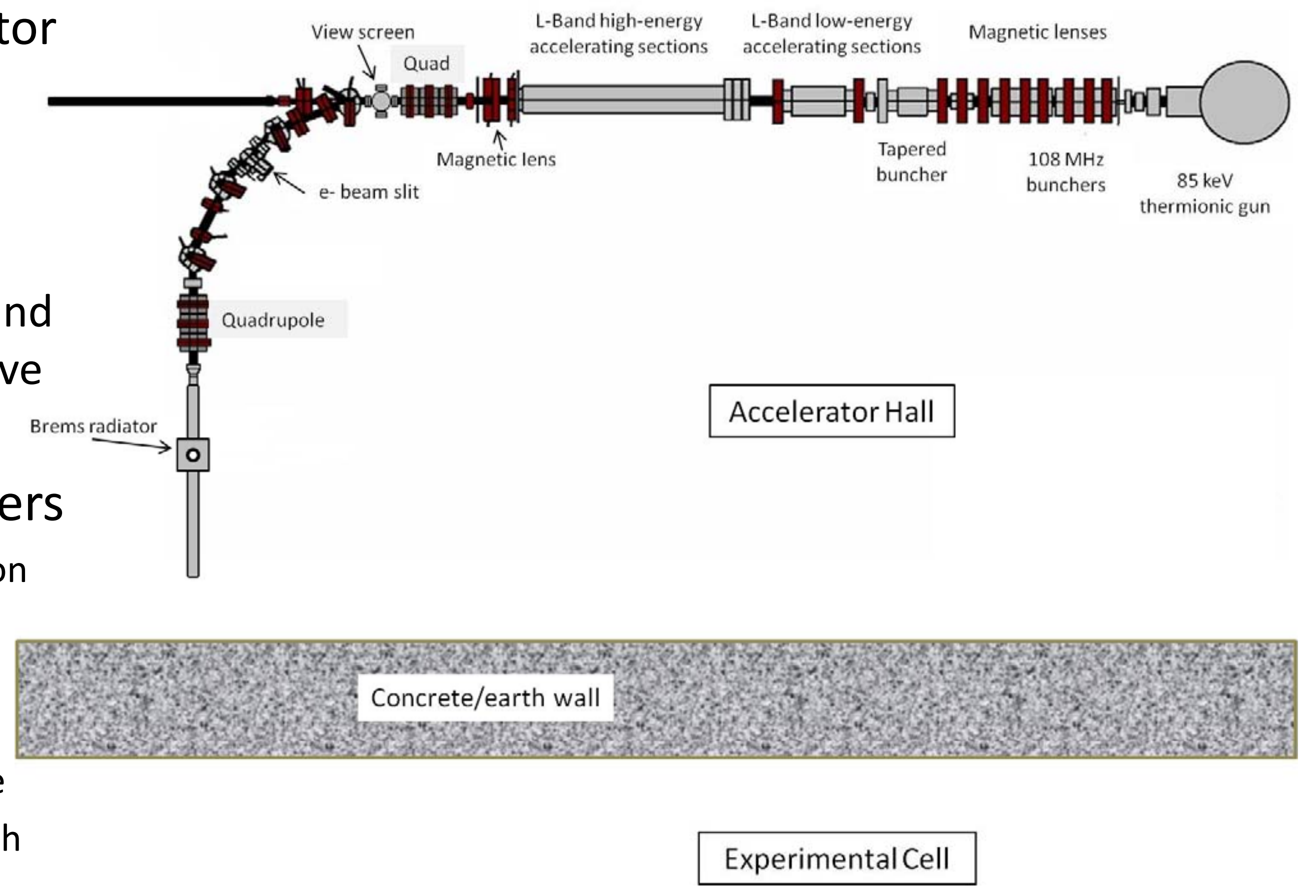

Figure 8: Schematic of the layout of the 44 MeV short pulsed linac at the Idaho Accelerator Center.

Bremsstrahlung Radiator

Figure 9: ½ mil Al radiator attached to a ladder.

- ½ mil (1.4×10^{-4} r.l.) thin Aluminum foil
  - Minimizes multiple scattering
- Sandwiched between 2mm thick aluminum plates
- In/out ability using ladder

- Highest degree of polarization within the bremsstrahlung cone has been shown [3,4] to be at

$\theta_c = m_e c^2 / E_{beam} = 1.17°$

  - m_e = 0.511 MeV
  - E_{beam} = 25 MeV

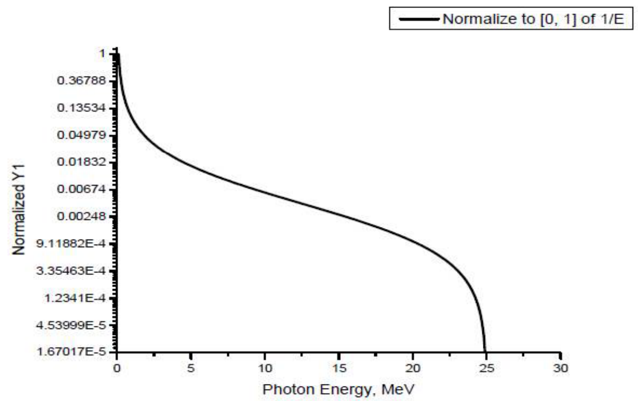

Figure 10: Bethe-Heitler distribution of bremsstrahlung photons for a 25 MeV electron beam.

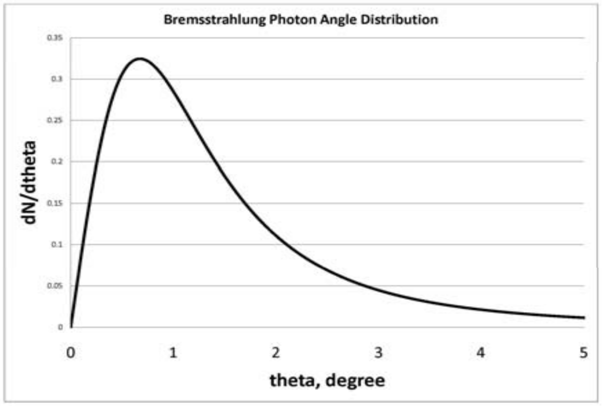

Figure 11: Angular distribution of bremsstrahlung for 25 MeV electron beam.

1. U E P Berg and U Kneissl. Recent progress on nuclear magnetic dipole excitations. Annual Review of Nuclear and Particle Science, 37(1):33-69, 1987
2. Haakon Olsen and L. C. Maximon. Photon and electron polarization in high-energy bremsstrahlung and pair production with screening. Phys. Rev., 114(3):887-904, May 1959.

Off-Axis Bremsstrahlung

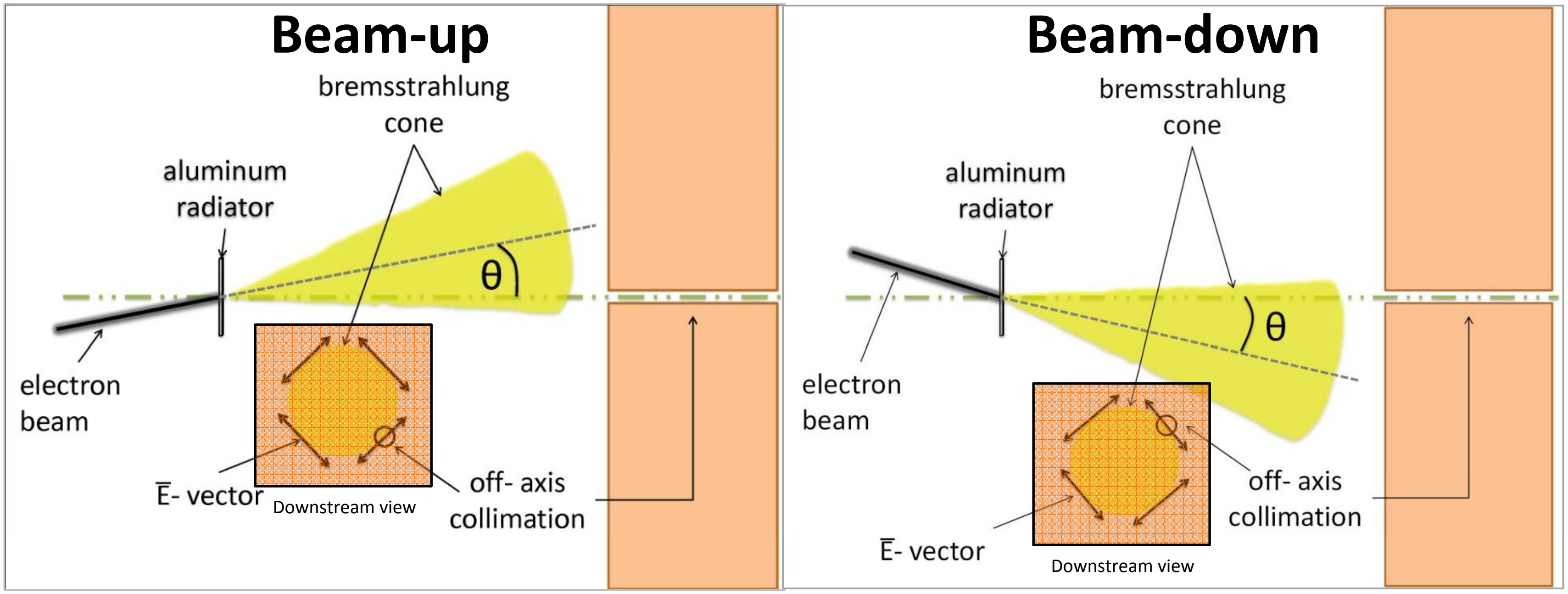

Figure 12: A schematic of the setup used to produce linearly polarized photons via the off-axis bremsstrahlung technique. Two cases of polarization will be provided.

- Off-axis bremsstrahlung is partially linearly polarized
  - Electric field vector lies preferentially perpendicular to the emission plane of photons aligned tangentially to a circle around incident beam direction
  - Off-axis collimation system was designed such that all of the bremsstrahlung cone blocked except a small portion at an angle $\theta_c = m_e c^2 / E_{beam}$, with respect to the center of the cone
    - This fixed collimation allows for two polarization states

Off-Axis Collimation

- Linearly polarized photons in the experimental cell
  - Want nothing else
- Off-axis collimation
- Two iron collimators
  - 15cm thick
  - 11 MeV (γ,n) threshold
- Upstream
  - 2cm diameter hole drilled 4.1cm beam right of central hole
- Downstream
  - 4cm diameter hole drilled 6.8cm beam right of central hole
- Kicking electron beam up (down) before radiator polarized photon beam with $\vec{E} \rightarrow$ -45° (+45°)

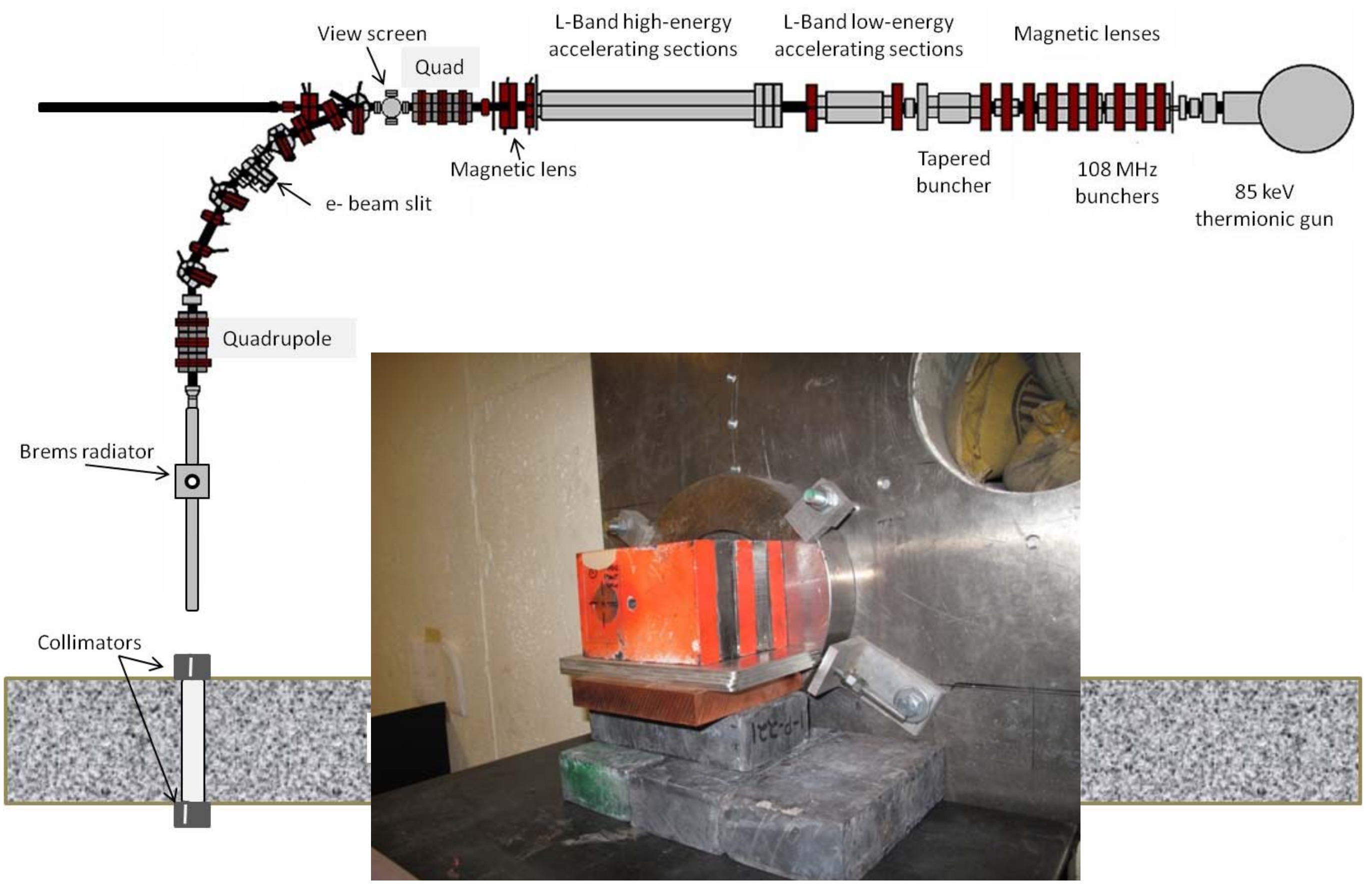

Figure 13: Off-axis collimation used to transport linearly polarized bremsstrahlung into the experimental cell for experimentation.

Beam Position Control

Kicker magnets used to steer the electron beam

- Two magnetic coils were secured to the beam pipe upstream of the radiator
- Powered using a high current power supply, which is remotely controlled from the counting room
  - Provides a means of switching polarity without a obtaining a hall access
  - Two polarization states
    - Beam-up
    - Beam-down

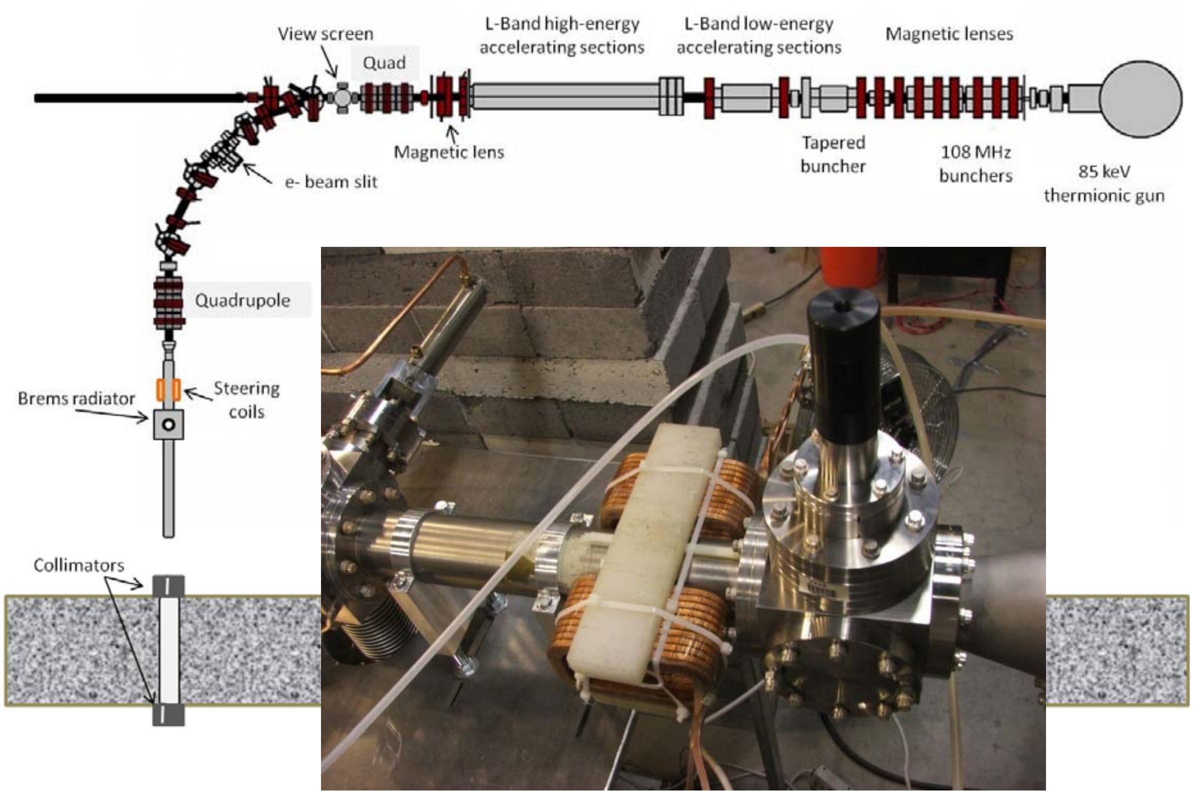

Figure 14: Electromagnetic coils used to steer the electron beam such that the beam is incident upon the radiator at an angle of 0.83°, giving way for linearly polarized photon beam into the experimental cell.

Kicker Magnet Angle

- Angle at which the electron beam strikes the radiator (θ_k)is crucial
  - Determines polarization
- Off axis collimation $\theta_c/3$ acceptance
- Distances
  - Radiator to collimator: 286 cm
  - Laser hole to center of off-axis collimation hole: 4.13 cm
  - Brems cone center to center of off-axis collimation hole: Δ_1
  - $\theta_c = m_e c^2 / E_{beam} = 1.17°$
    - Δ_1=5.85 cm
  - θ_k= 0.83°

  - For maximum polarization the electron beam needs to strike the radiator at an angle

    θ_k= 0.83°

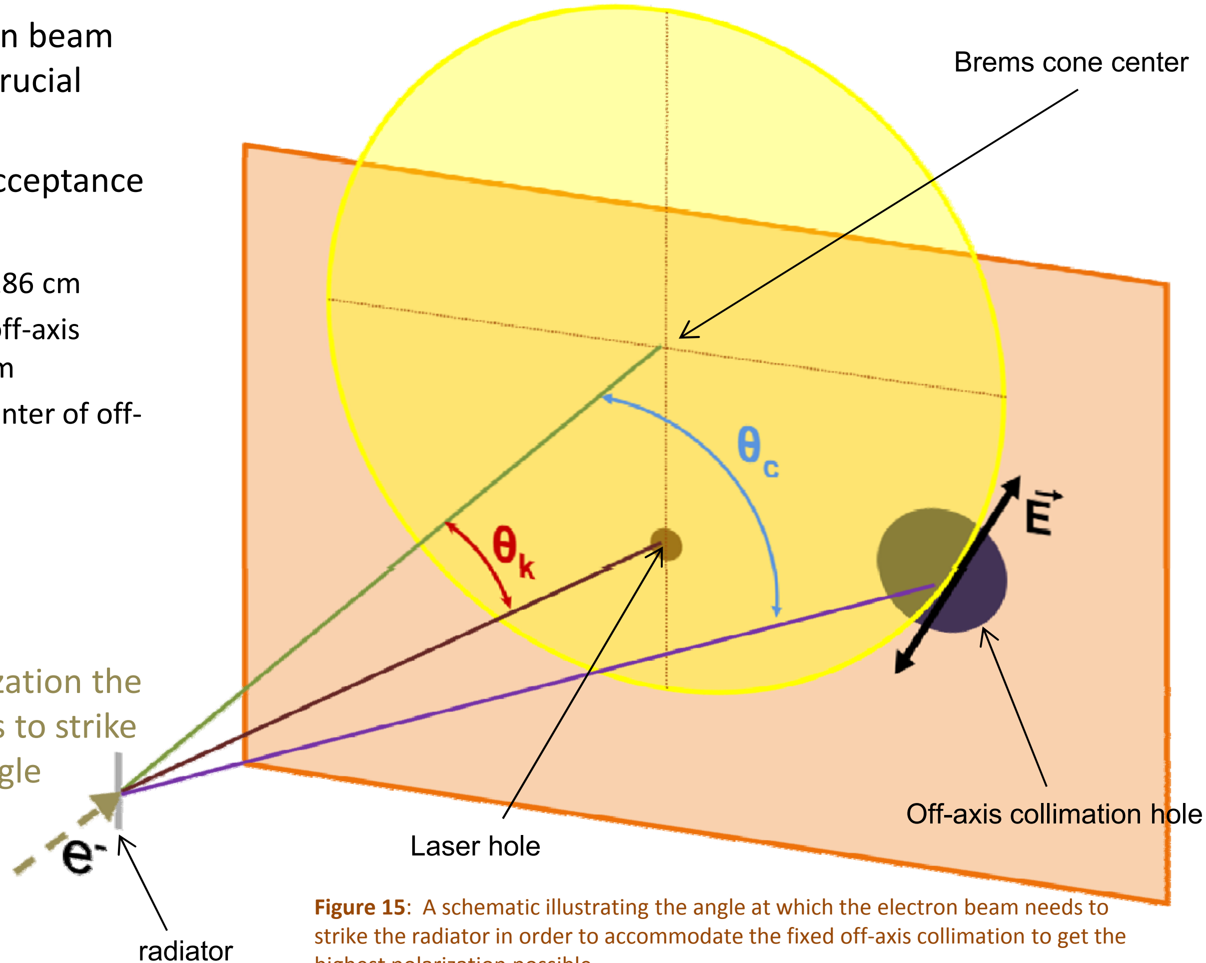

Figure 15: A schematic illustrating the angle at which the electron beam needs to strike the radiator in order to accommodate the fixed off-axis collimation to get the highest polarization possible.

Beam Position Monitoring

- Faraday cup used to
  - Monitor the electron beam position
  - Electron beam divergence (to an extent)
  - Kicker magnet calibration tool
- Faraday cup is made of 70 square aluminum rods
  - 6mm x 6mm x 75mm
  - Spaced 1.4mm apart
  - The back side of each brick is a wire that leads to the data acquisition
  - Each brick is assigned its own ADC
  - Data are recorded such that the more charge deposited onto a brick in a time δt, the higher the channel number the data is assigned to

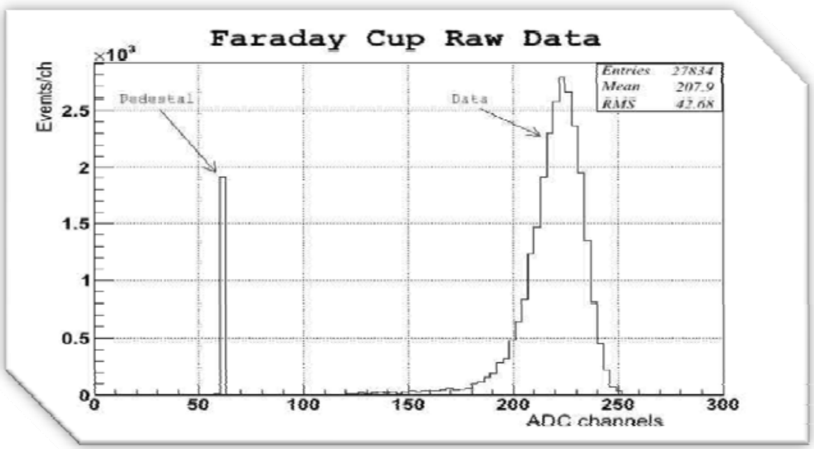

Figure 16: ADC spectrum of one pixel of the Faraday cup illustrating the calibration point (pedestal) and the data (collected charge).

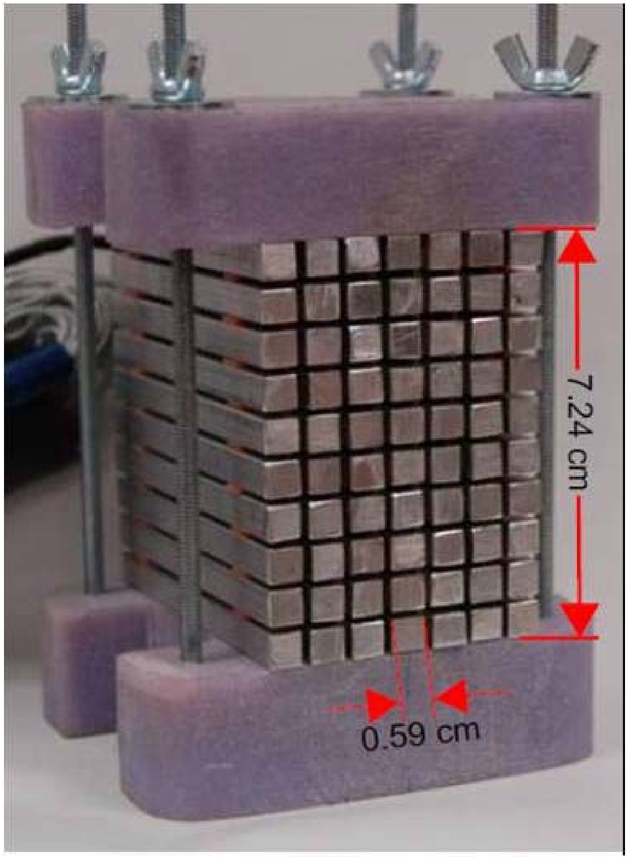

Figure 17: Faraday cup designed to monitor the electron beam position for calibration of the kicker magnets.

Faraday Cup-Data Analysis

How to analyze the data:

- ADC calibrated by subtracting the pedestal from the data
- Integrate peak
  - Proportional to charge
- Center of gravity technique
  - On a **pulse by pulse** basis, the charge of each pixel is weighted by the total charge of the whole FC, thus finding the average beam position each pulse as

$$X_{avg}^{pulse} = \frac{\sum (Q_i * x_i)}{\sum Q_i}$$

  - Q_i is the charge in the i^th pixel
  - Distribution over **all beam pulses**, the average beam position is found as

$$X_{AVG} = \frac{\sum_{i=1}^{\# pulses} X_{avg}^{pulse}}{\# pulses}$$

  - Absolute error is found as

$$X_{error} = \sqrt{\frac{1}{\# pulses} \sum_{i=1}^{\# pulses} \left(X_{avg}^{pulse} - X_{AVG}\right)^2}$$

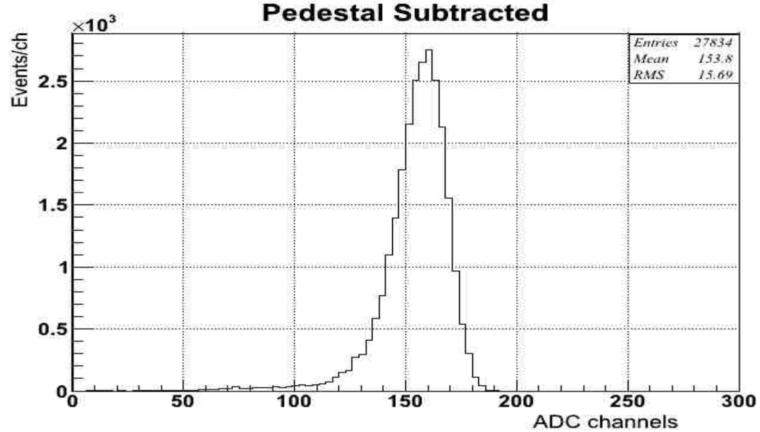

Figure 18: An example of an ADC spectrum from one pixel of the Faraday cup with the pedestal correction applied.

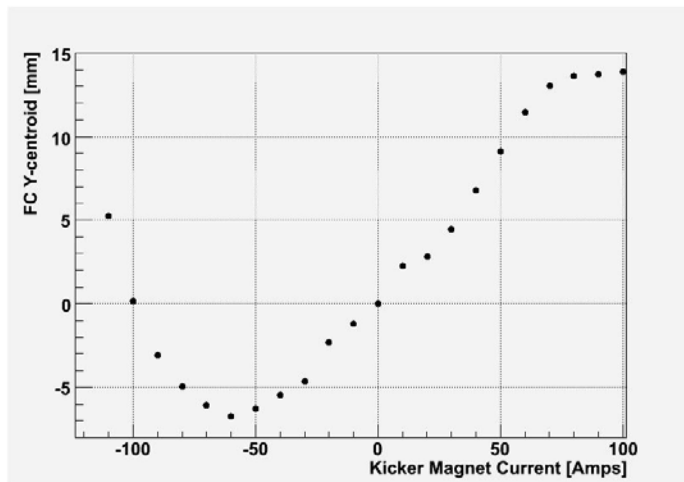

Figure 19: Faraday cup data analysis results using a center of gravity technique. The results show that the Faraday cup is too small for this experimental setup.

What happened?

- e- beam too dispersed at this point
- Faraday cup is too small for this setup
  - Designed for HRRL which has much more compresses geometry
- Larger FC in the works

Zinc Sulfide View Screen Method

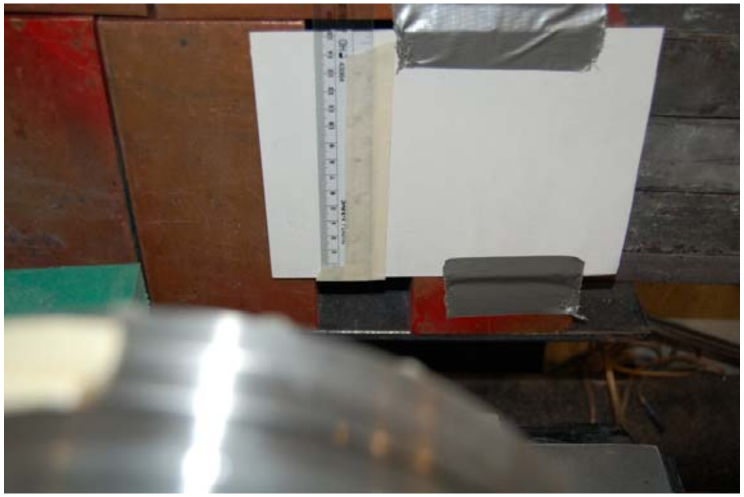

Figure 20: A picture of how the zinc sulfide view screen was used to calibrate the kicker magnets.

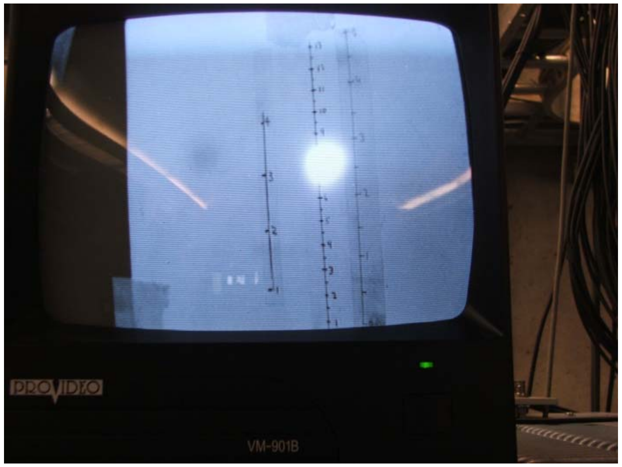

Figure 21: A picture showing the zinc sulfide view screen glowing as electrons hit it.

- The zinc sulfide view screen
  - Thin plastic sheet, 1mm, covered in a layer of zinc sulfide
- Electrons incident upon zinc sulfide scatter, resulting in a glowing spot on the view screen
  - Electron transitions-phosphorescence
- Monitor from counting room using a video camera

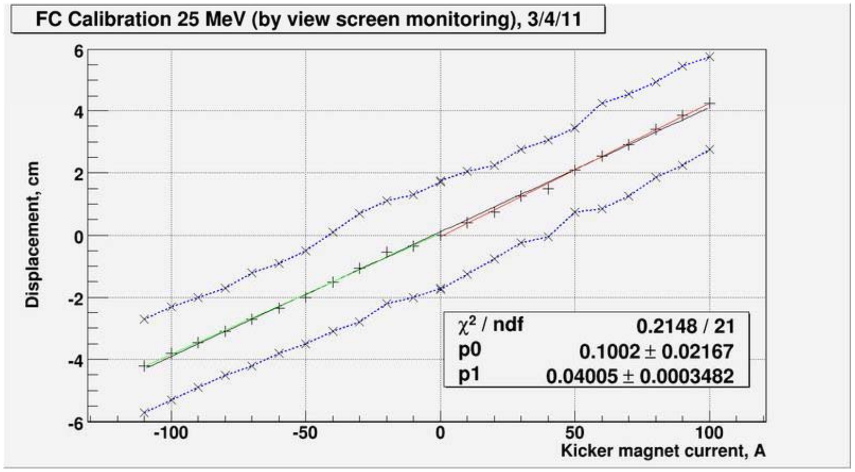

Figure 22: The calibration curve illustrating the bending action of the kicker magnets as a function of current.

Removal of Charged Particles

Figure 23: Charged particles are swept from the beam line using a 3kG x 20cm permanent magnet, and dumped into a graphite and lead beam dump.

- Charged particles are
  - swept from the beam line using a 3 kG x 20 cm permanent dipole
  - dumped into beam dump
    - 10 cm graphite
    - 15 cm lead
- Providing a cleaner linearly polarized photon beam sent into the experimental cell

Photon Flux

- Importance of photon flux
  - Expected rates
    - How long experiment will take
  - Used for neutron count rate normalization between two polarization states
    - D_2O background subtractions
- Flux expected in experimental cell can be calculated
  - Depends upon
    - Electron beam
      - Current
      - Pulse width
      - Repetition rate
    - Photons produced in radiator
    - Energy of photons
    - Radiator thickness
    - Collimation factor

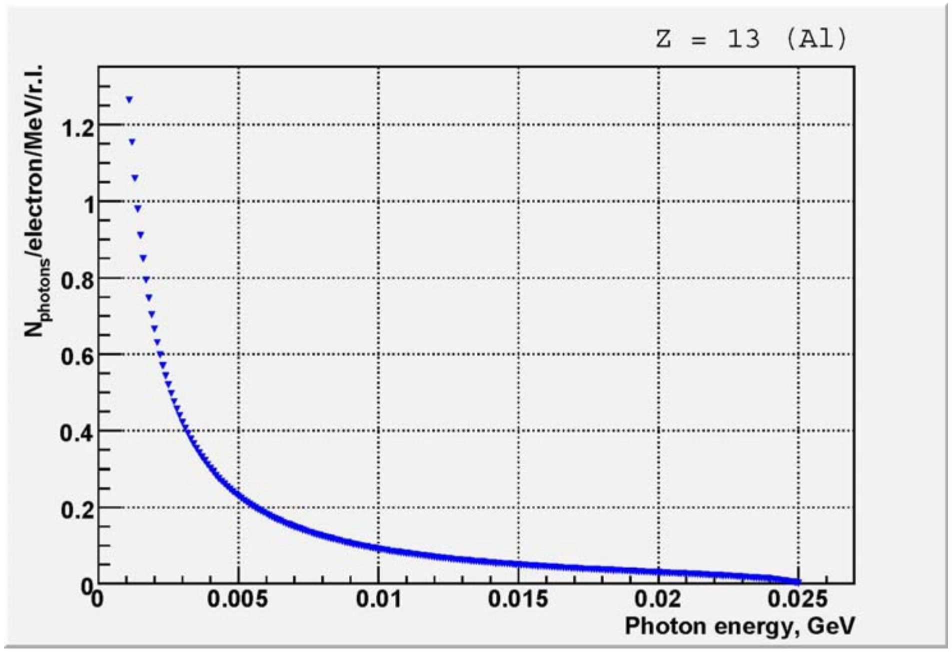

Figure 24: A calculation showing the number of photons produced in the aluminum radiator via bremsstrahlung [5] .

$$flux = 0.2\frac{\gamma' s}{e^- \cdot MeV \cdot r.l.} \times 1.4\cdot 10^{-4} r.l. \times 5MeV \times 9.375\times 10^{11}\frac{e^-}{s} = 2.6\cdot 10^{8}\frac{\gamma}{s}\times 0.5c.f. = 1.3\cdot 10^{8}\frac{\gamma}{s}$$

- Too many parameters that can change
- Much easier if we had something to monitor this for us

[5] J.L. Matthews and R.O. Owens. Accurate formulae for the calculation of high energy electron bremsstrahlung spectra. Nuclear Instruments and Methods, 111(1):157-168, 1973.

The Pair Spectrometer

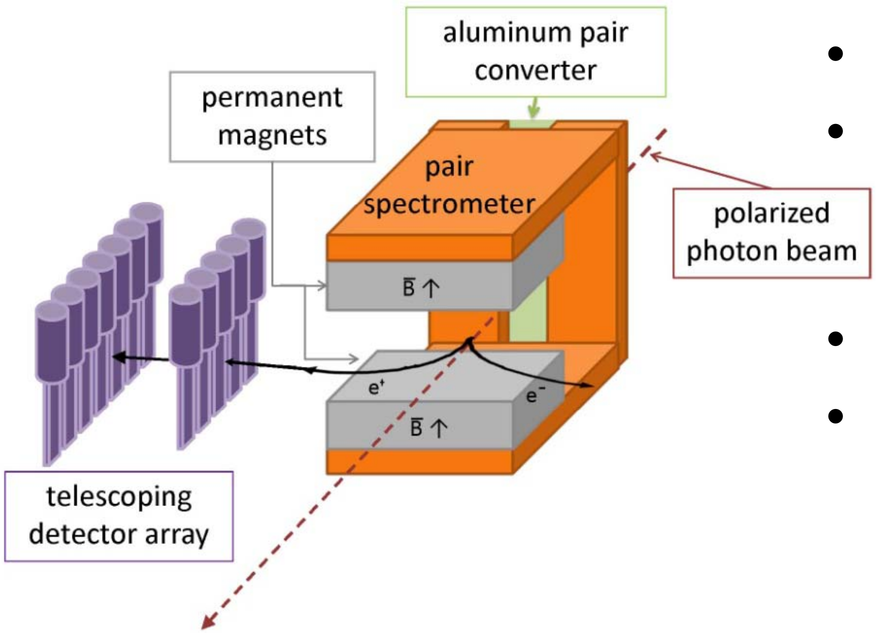

Figure 25: A pair spectrometer designed to be used a s a relative photon flux monitor.

- Fraction of the photon beam pair-produces
- e^+/e^- separate trajectories
- Detecting positrons using telescoping detectors
  - Less background e^+ than e^-
- Independent of polarization
- Use as relative normalization factor in neutron asymmetry calculations

Relative Photon Flux Monitor

Preliminary Run

Figure 26: Pair spectrometer being tested at the Idaho Accelerator Center, September 2011.

- September 2011, tested at the IAC
  - Didn't use the whole array of detectors (preliminary test)
  - Very sensitive to background
    - Requires heavy shielding
- Functioned well as a beam stability monitor
  - Real time monitoring allowed us to see when beam was lost
    - Due to accelerator issues, operator error, etc.

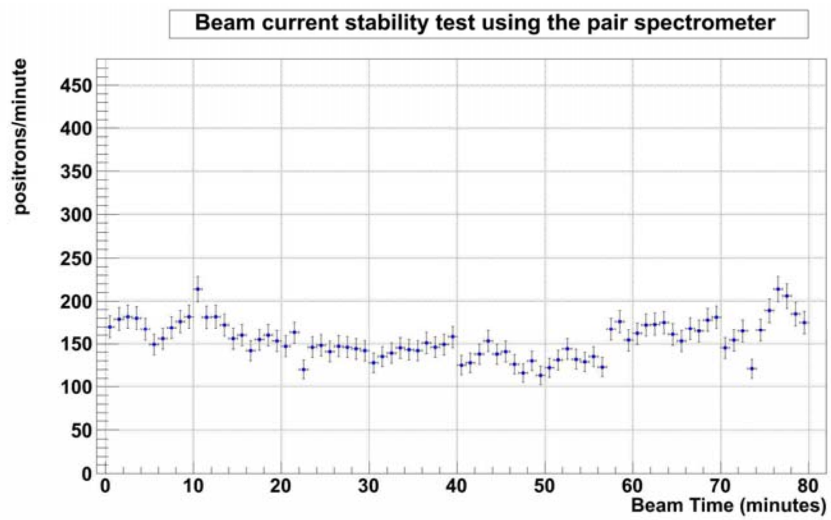

Figure 27: Results of a preliminary test using the pair spectrometer as a beam stability monitor Idaho Accelerator Center, September 2011. The results shown have a bin width of 1 minute, indicating that the beam current is not very stable.

Neutron Detector Setup

- 3 neutron detectors are set perpendicular to incident beam at angles for asymmetry measurements
  - Corresponding to +/- 45° E-field vector
  - Covered in
    - 4 inches lead
    - 4 inches poly

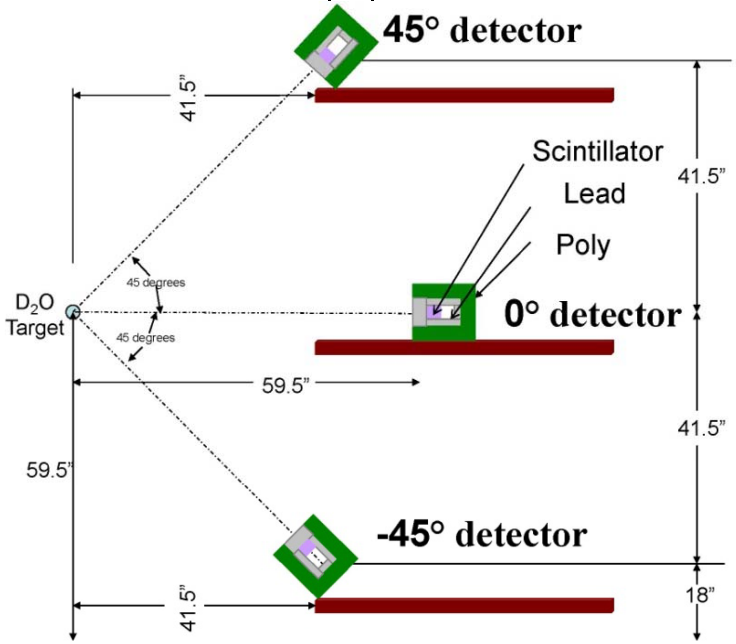

Figure 28: Neutron detector setup for neutron asymmetry measurements.

Figure 29: Neutron detector setup for a preliminary run at the Idaho Accelerator Center, March 2011.

- The upper and lower detectors will be used for asymmetry measurements
- The middle detector can be used as a relative flux normalization detector
  - Independent of polarization

- Now, the linearly polarized γ-ray beam established
  - Discuss how to measure the polarization

"You are completely free to carry out whatever research you want, so long as you come to these conclusions."

Determining Polarization

Can measure polarization by ɣ(D,n)p

- Threshold is at binding energy 2.2 MeV
- Process can be either
  - Photomagnetic $^3S \rightarrow {}^1S$
    - Angular distributions are isotropic
  - Photoelectric $^3S \rightarrow {}^3P$
    - Angular distribution has a normal dipole distribution with respect to the electric field vector of the photon

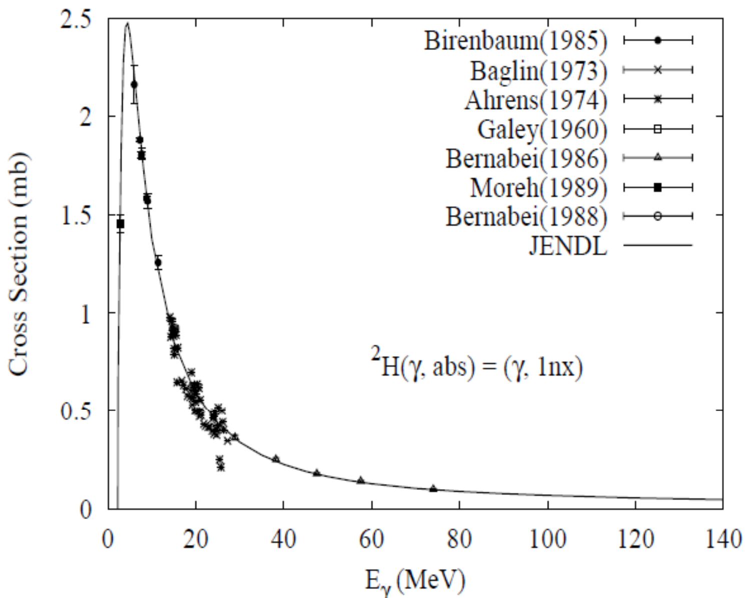

Figure 30: Photodisintegration cross section of the deuteron[6].

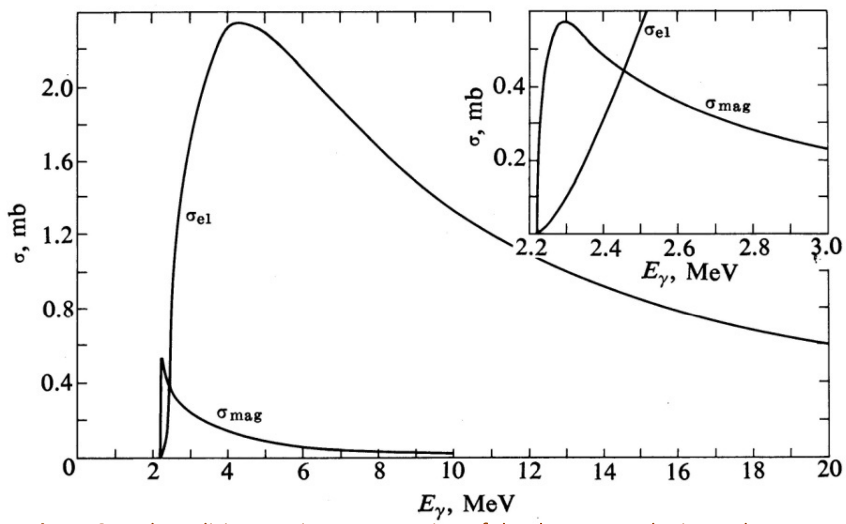

Figure 31: Photodisintegration cross section of the deuteron. The inset shows a close-up of the region by the threshold energy[7].

Cross sections reveal:

- Small magnetic dipole contribution around threshold
- Electric dipole transitions dominate above threshold

[6] Handbook on Photonuclear Data for Applications Cross-sections and Spectra, © IAEA, 2000, pg.95
[7]Emilio Segre. NUCLEI AND PARTICLES: An Introduction to Nuclear and Subnuclear Physics. W. A. BENJAMIN, INC., 1964.

Analyzing Power

Asymmetry measurements with linearly polarized photons yields analyzing power

- Defined as:

$$A(\theta,E_\gamma)=\frac{1}{P_\gamma(E_\gamma)}\frac{\sigma_\perp(\theta,E_\gamma)-\sigma_\parallel(\theta,E_\gamma)}{\sigma_\perp(\theta,E_\gamma)+\sigma_\parallel(\theta,E_\gamma)}$$

  - $\sigma_\perp$ (σ): cross sections for photons polarized perpendicular (parallel) to polarization plane at scattering angle θ and excitation energy E_γ

- Studied at emission angle θ=90°
- 10 MeV » near unity

Polarization simplifies to

$$P_\gamma=\frac{d\sigma_\perp-d\sigma_\parallel}{d\sigma_\perp+d\sigma_\parallel}$$

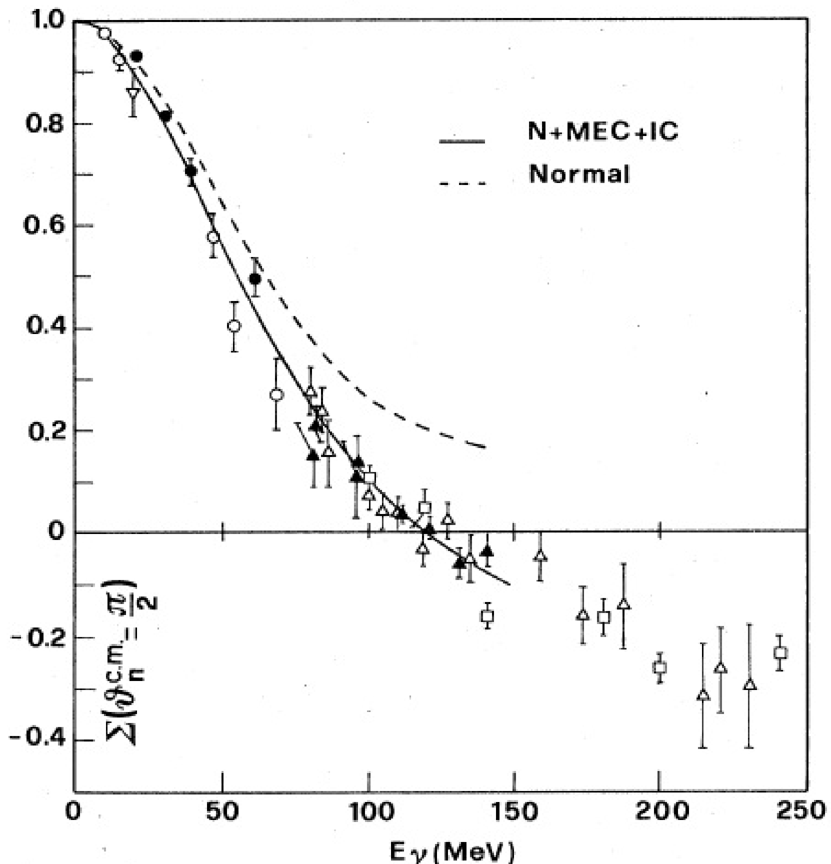

Figure 32: Theoretical and measured analyzing power of photodisintegration of the deuteron[8]. The dashed line corresponds to the standard Partovi approximation; the solid line reflects the inclusion of meson exchange currents MEC and nucleon isobar contributions (IC) corrections.

[8] M. P. De Pascale, G. Giordano, G. Matone, D. Babusci, R. Bernabei, O. M. Bilaniuk, L. Casano, S. d'Angelo d'Angelo, M. Mattioli, P. Picozza, D. Prosperi, C. Schaerf, S. Frullani, and B. Girolami. Polarization asymmetry in the photodisintegration of the deuteron. Phys. Rev. C, 32(6):1830-1841, Dec 1985.

Polarization Measurement

Figure 33: D_2O target used to measure the polarization of the off-axis bremsstrahlung beam.

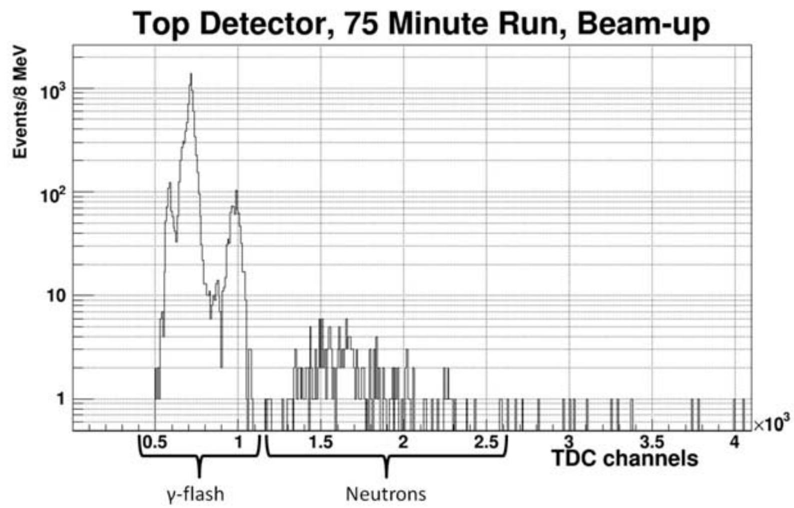

Figure 34: An example of the TDC spectra gathered during a run using a 25 MeV electron beam incident upon an aluminum radiator, collimating the bremsstrahlung photons which are incident upon a D_2O target.

Photodisintegration of the deuteron

- Using a highly sophisticated D_2O target
  - Plastic bottle filled with 500ml D_2O
    - 90% enriched
  - 6cm diameter
  - 20cm long
- Measured neutron asymmetries
  - Two polarization states

TDC Spectrum

- Gamma flash
- Continuum of neutrons
  - Structure within gamma flash
    - Which peak is target related?
    - Removed lead, target in/out test
    - What are the other peaks from?
    - Converted to distance scale…

Neutron Energy Spectrum

Using the time of flight technique, the gamma flash from the deuterium can be used to determine the energy of the neutrons

- How this works:
  - Photons travel at c
    - 30 cm per ns
    - D_2O γ-flash is calibration point
  - 1 MeV neutrons 5% of c
    - 1.5 cm per ns
  - 5 MeV neutrons 10% of c
    - 3 cm per ns
  - Top detector is 146 cm away from the target
    - 1 MeV neutrons arrive 90 ns after γ-flash
    - 5 MeV neutrons arrive 50 ns after γ-flash
  - Can convert TDC spectrum into neutron energy

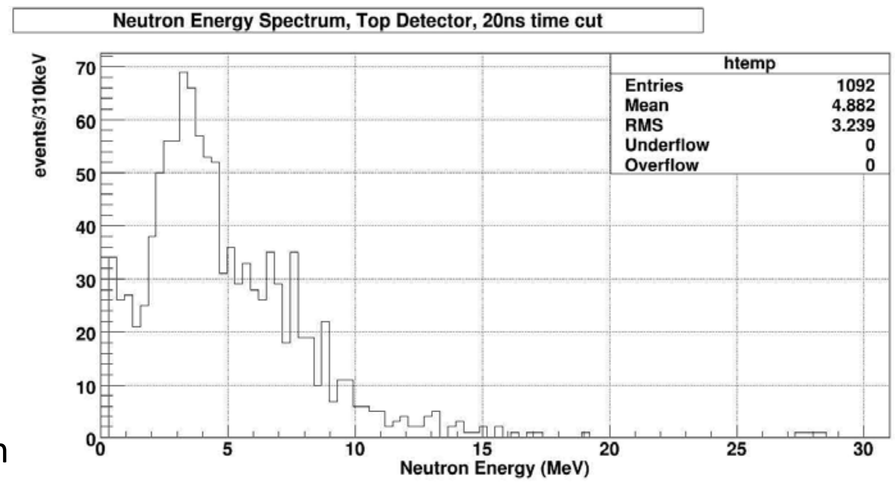

Figure 35: The energy spectrum of the detected neutrons from photodisintegration of the deuteron using the time of flight technique.

Using 2-body kinematics to find the approximate photon energy:

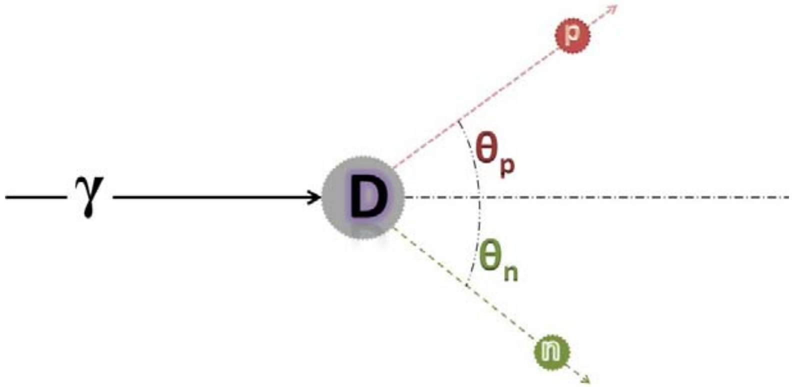

Figure 36: Schematic of the two body reaction D(γ,n)p.

•Apply the conservation of momentum

$p_\gamma + p_D = p_n + p_p$

•Solving for incident photon energy as a function of neutron energy we get

$T_\gamma = 2.003 T_n + 1.715$

•4-momentum vectors:

- $p_\gamma = (T_\gamma, T_\gamma, 0, 0)$
- $p_D = (m_D, 0, 0, 0)$
- $p_n = (E_n, p_n \cos\theta_n, p_n \sin\theta_n, 0)$
- $p_p = (E_p, p_p \cos\theta_p, p_p \sin\theta_p, 0)$

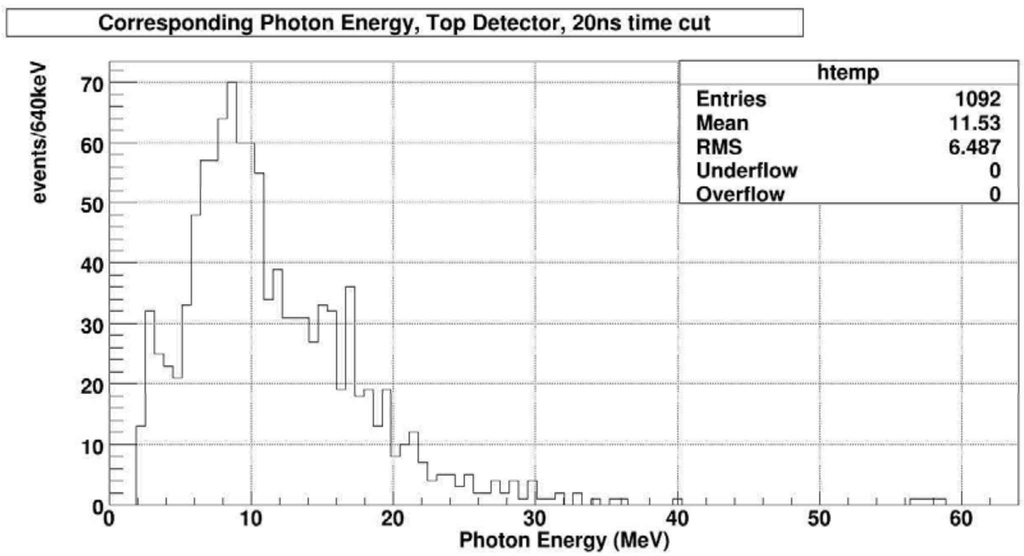

Figure 37: An energy spectrum of the photons corresponding to the neutron spectrum from photodisintegration of the deuteron.

The Asymmetry Calculations

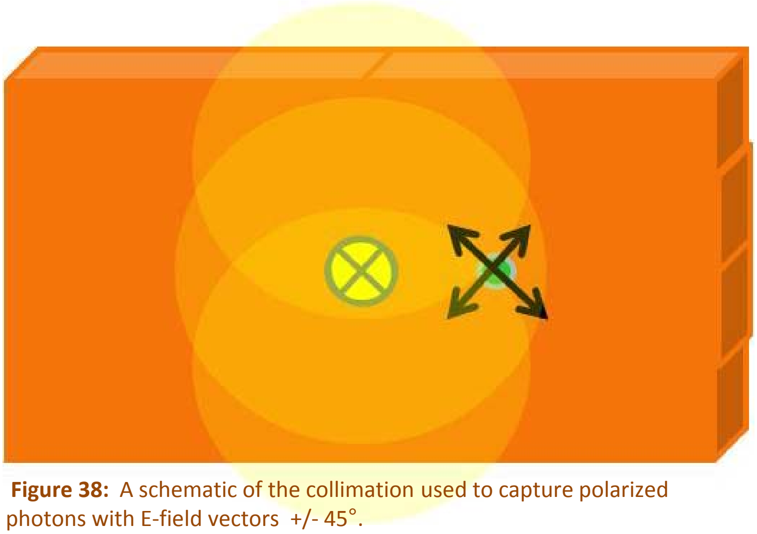

Figure 38: A schematic of the collimation used to capture polarized photons with E-field vectors +/- 45°.

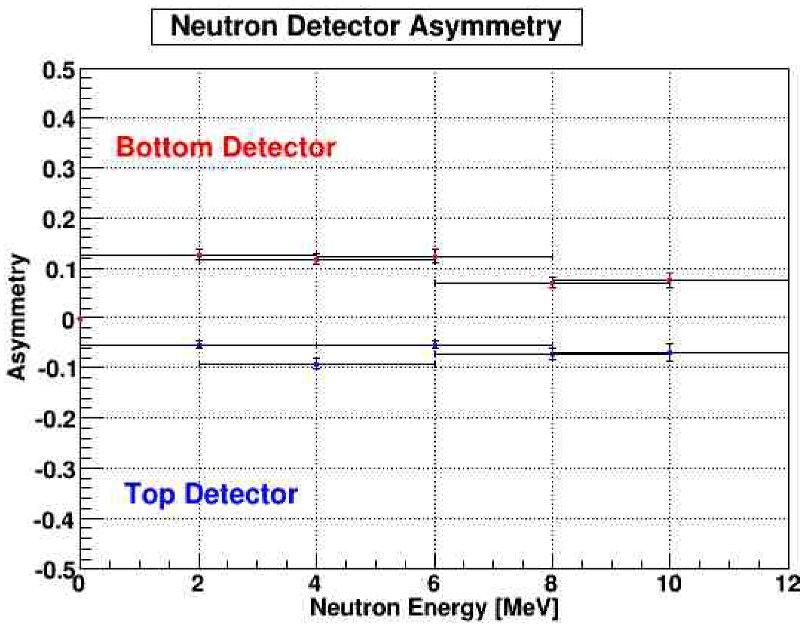

Figure 39: Measured neutron asymmetries for photodisintegration of the deuteron using linearly polarized photons.

- Two polarization states
  - beam-up
  - beam-down
- For each detector, the asymmetry is found as

$$Asy = \frac{(\# n^{\circ}_{beam-up}) - (\# n^{\circ}_{beam-down})}{(\# n^{\circ}_{beam-up}) + (\# n^{\circ}_{beam-down})}$$

  - where $\# n^{\circ}$ represent the number of neutrons detected normalized to the total number of neutrons detected in the middle detector (0°).

Results:

- Expected sign!
- Vary from 12% to 5%
- Look at cumulative asymmetry

Running Asymmetry

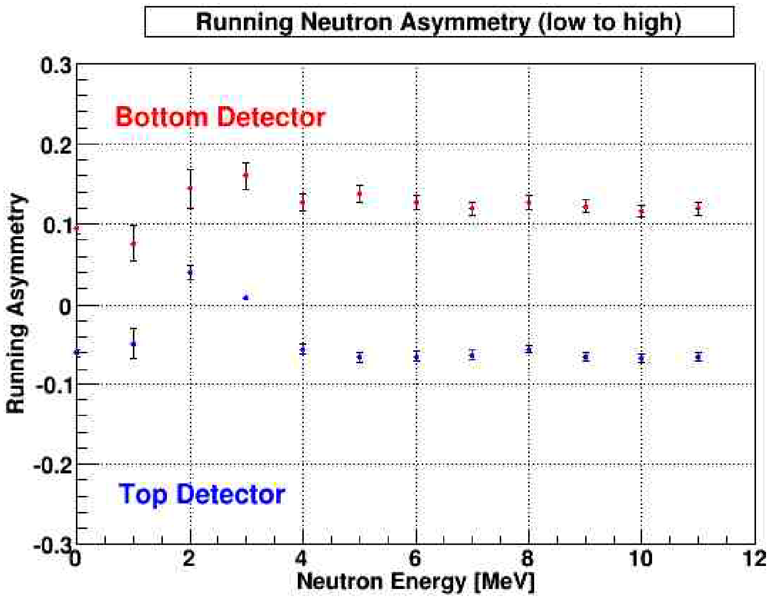

Figure 40: Running asymmetry used to gather more statistics where each bin is added to the next in a cumulative fashion starting from 0 MeV.

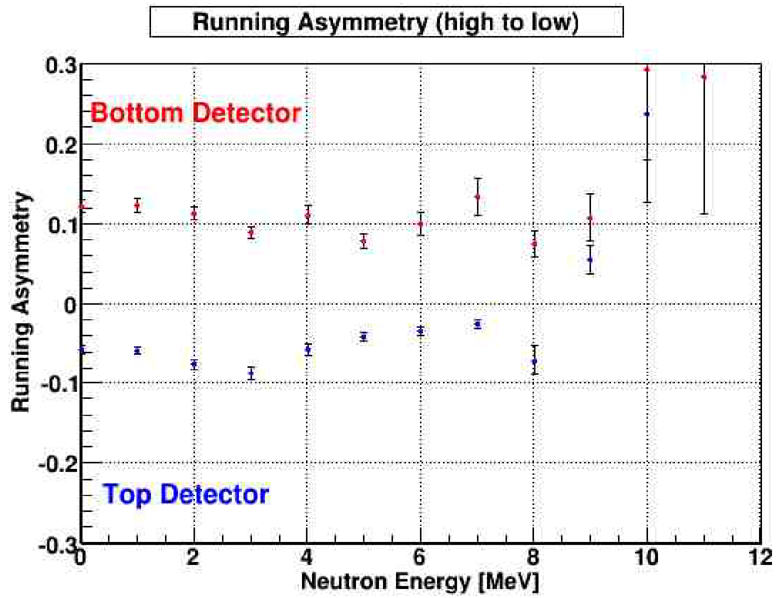

Figure 41: Reverse cumulative asymmetry where each bin is added to the next in a reversely cumulative fashion starting from 12 MeV.

- Here each bin added to the next in a cumulative fashion
  - Starting from
    - 0 MeV for low to high
    - 12 MeV for high to low
  - Most statistics are in the 2-5 MeV range
  - Really low statistics at higher energies (>8 MeV)

Polarization

- Top detector ~7% asymmetry
- Bottom detector ~ 10% asymmetry

- Polarization is roughly **8.5%**

- Previous experimenters[3] and theoretical calculation[4] indicate a 30% polarization

Why lower polarization?

- Low Statistics
  - 0.1 Hz neutron detection rate
- Kicker magnet calibration
  - Geometry error
- Instability of electron beam
  - Beam wandering off the radiator
- Photodisintegration of the deuteron cross section peaks about E_γ=5 MeV, which corresponds to E_n = 1.5 MeV
  - What about neutron scattering within the target?

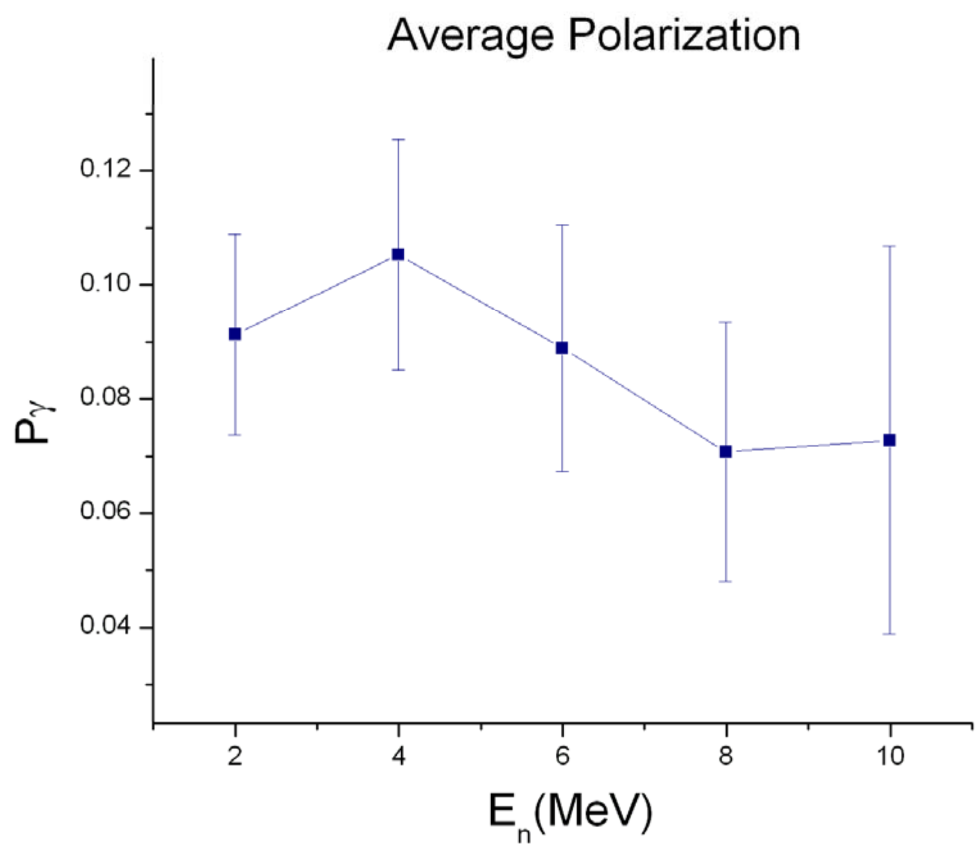

Figure 42: Polarization of the gamma-ray beam plotted as a function of neutron energy. Determined via photodisintegration of the deuteron.

[3] U.E.P. Berg and Ulrich Kneissl, Ann. Rev. Nucl. Part. Sci. 37, 33-69 (1987)

Polarization Remarks

- Neutrons scattering within D_2O target?
  - Angular asymmetry washed out
- MCNPX simulation
  - Pencil beam of 1 MeV neutrons generated inside a 6 cm diameter container of D_2O initially directed towards the detector
  - Segmented detector measures the angular distribution of neutrons after exiting the D_2O.

Results:

1 MeV neutron scattering in D_2O is negligible.

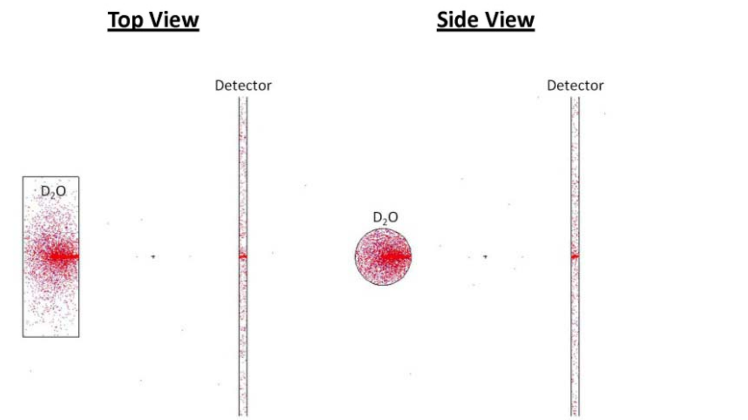

Figure 43: Setup of MCNPX simulation used to see the scattering effects 1 MeV neutrons encounter in D_2O.

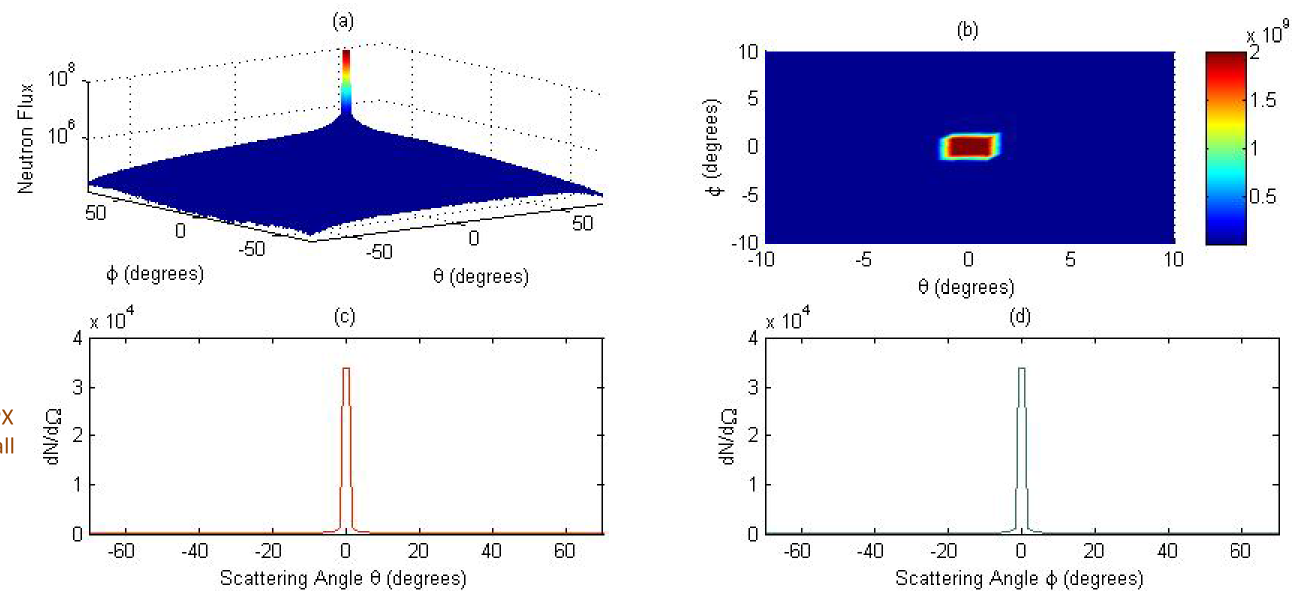

Figure 44: Results of MCNPX simulation showing the small scattering effects 1 MeV neutrons encounter in D_2O.

Polarization Remarks (continued…)

- Recall the size of the electron beam according to the zinc sulfide screen
  - 3 cm diameter
- Radiator is only 2.5 cm in diameter
  - Beam scrapping on radiator holder (4mm thick)
    - Compared to ½ mil (12.5μm) radiator
  - Affecting polarization measurement results

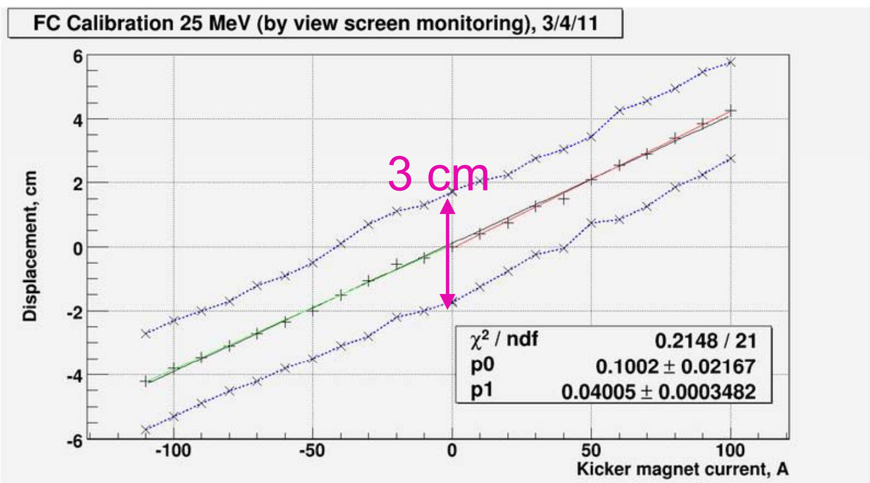

Figure 45: Electron beam size as seen on the zinc sulfide view screen, use in calibrating the kicker magnets.

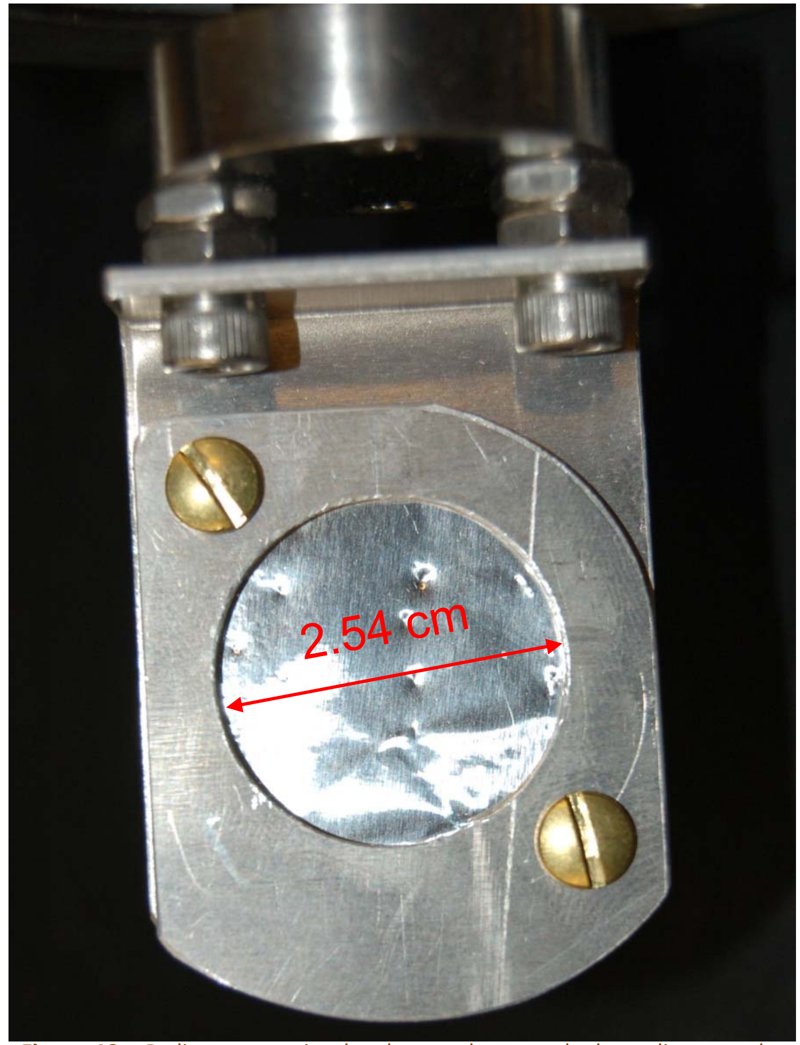

Figure 46: Radiator mounting bracket used to attach the radiator to the ladder to provide an in, or out, or the beam ability. Measurements reveal the inner diameter of the holder may be interfering with the electron beam.

Future Work

- Modify the bremsstrahlung radiator
  - Try 4mm horizontal strip held by thin wires (done Sept 2011)
- Enlarge Faraday cup
  - Increase spacing between pixels
- Neutron detector enhancement
  - 180° capability (done Sept 2011)
  - Lots of shielding! (done Sept 2011)
- Use HRRL
  - Higher rates, more statistics
  - More stable beam
- Detection of prompt neutrons from photofission of actinides
  - Oleksiy Kosinov's PhD. project
  - Implement for homeland security and safeguard applications

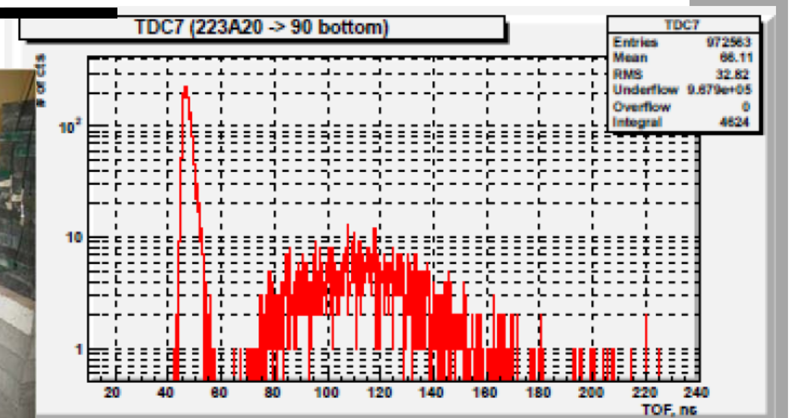

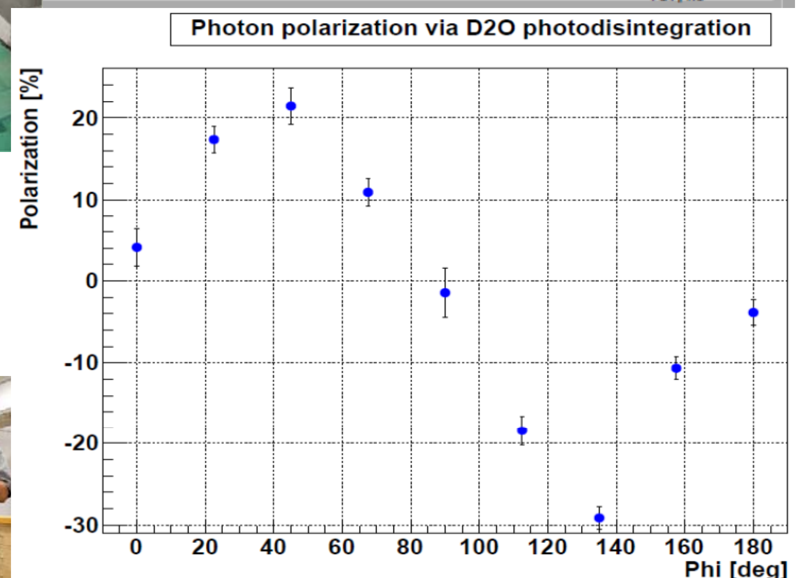

P(φ) = [Up(φ)/sumUp(φ) - Down(φ)/sumDown(φ)]/[..+..]

Summary

- A linearly polarized photon beam was established for photofission experiments
  - A segmented Faraday cup was designed and used to monitor the position of the electron beam
  - An off-axis collimation system was used to get a linearly polarized photon beam to the experimental cell
  - A pair spectrometer was designed to be used as a relative photon flux monitor, but was found to be very useful as a beam stability monitor
  - The polarization of the photon beam was determined using photodisintegration of the deuteron
    - Found to be about 8.5% on average
- Minor modifications are needed for photofission experiments (Oleksiy's project)
  - Next run Spring 2012 using HRRL

Acknowledgements

- I would like to express my profound gratitude to my advisor Dr. Dale, for his immense help and guidance since taking on the task of being my advisor.
- I would also like to acknowledge the help I received from Dr. Valeriia Starovoitova during all stages of my research and the numerous hours spent trying to teach me MCNPX.
- I would also like to acknowledge Dr. McNulty for the help he provided with the data analysis.
- To my committee member, Dr. Forest, I would like to thank you for your help with this project and contributions to this thesis.
- To my graduate faculty representative, Dr. Ellis, I would like to thank you for your contributions.
- I would especially like to thank Oleksiy Kosinov for helping with every step of this project.
- I will also like to thank Roman Shapovalov and all the other collaborators who contributed to this project.
- And, last but not least, all the engineers at the Idaho Accelerator Center who worked in various ways to help move this project forward.

References

1. R. Ratzek et al. Photofission with Polarized Photons, Z. Phys. A.-Atoms and Nuclei. 1982, v. A308, p. 63-71.
2. C. Budtz-Jorgensen and H.-H. Knitter. Spontaneous investigations of fission fragments and neutrons in Cf-252. Nuclear Physics, A(490): 307-328, July 1988.
3. U E P Berg and U Kneissl. Recent progress on nuclear magnetic dipole excitations. Annual Review of Nuclear and Particle Science, 37(1):33-69, 1987
4. Haakon Olsen and L. C. Maximon. Photon and electron polarization in high-energy bremsstrahlung and pair production with screening. Phys. Rev., 114(3):887-904, May 1959
5. J.L. Matthews and R.O. Owens. Accurate formulae for the calculation of high energy electron bremsstrahlung spectra. *Nuclear Instruments and Methods*, 111(1):157-168, 1973.
6. Handbook on Photonuclear Data for Applications Cross-sections and Spectra, © IAEA, 2000, pg.95
7. Emilio Segre. NUCLEI AND PARTICLES: An Introduction to Nuclear and Subnuclear Physics. W. A. BENJAMIN, INC., 1964.
8. M. P. De Pascale, G. Giordano, G. Matone, D. Babusci, R. Bernabei, O. M. Bilaniuk, L. Casano, S. d'Angelo d'Angelo, M. Mattioli, P. Picozza, D. Prosperi, C. Schaerf, S. Frullani, and B. Girolami. Polarization asymmetry in the photodisintegration of the deuteron. *Phys. Rev. C*, 32(6):1830{1841, Dec 1985.

Thank You!

September 2011, Polarization

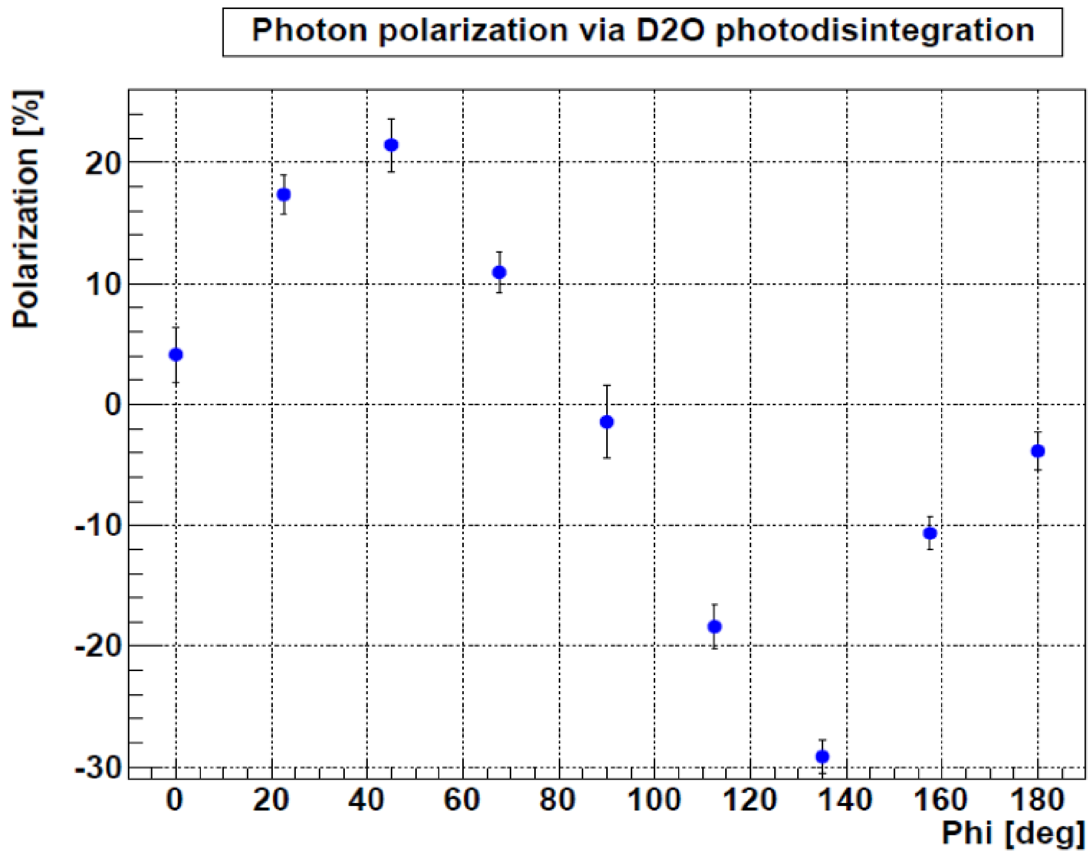

P(φ) = [Up(φ)/sumUp(φ) - Down(φ)/sumDown(φ)]/[..+..]

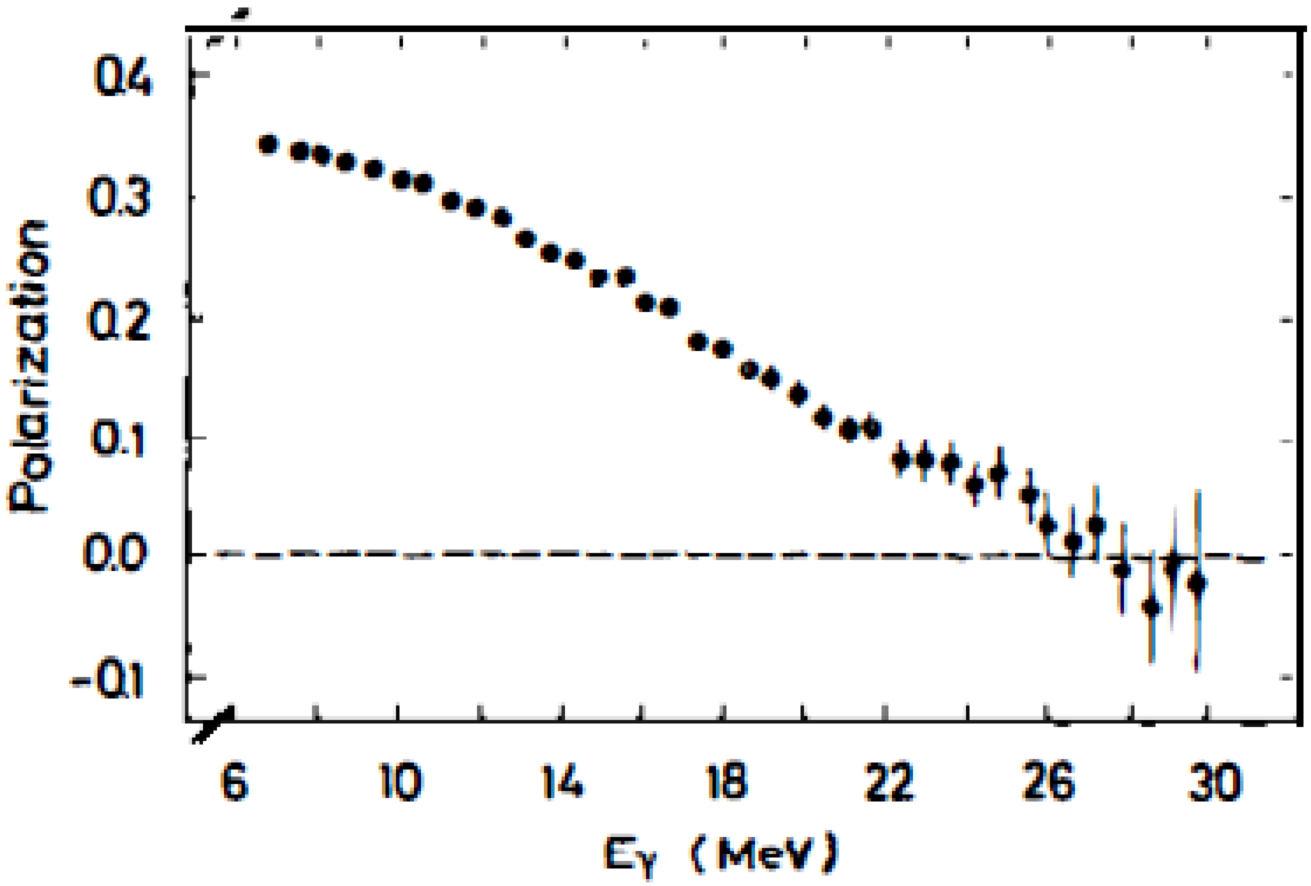

Degree of polarization of off-axis bremsstrahlung as a function of the photon energy (E_e = 30 MeV, θ = 1.4°)

C.F. Wienhard, K., Schneider, R. K. M., Ackermann, K., Bangert, K., Berg, U. E. P. Phys. Rev. C 24: 1363--66 (1981)

Try more vacuum…

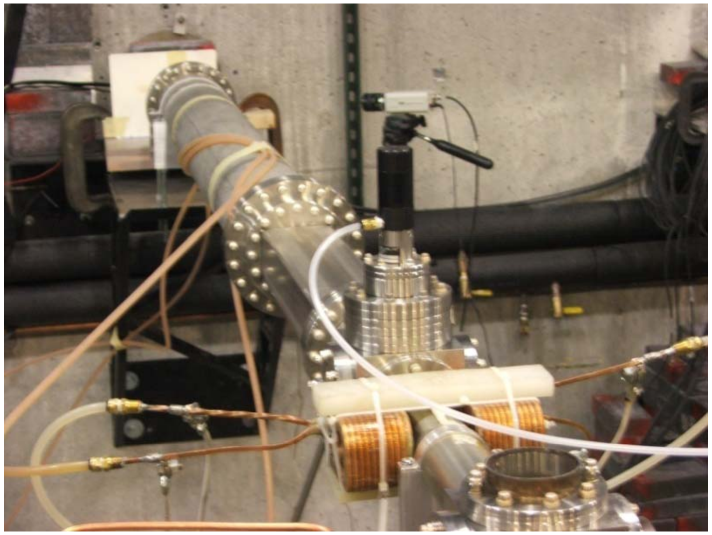

« upstream vacuum-pipe extension

Downstream vacuum pipe and sweep magnet

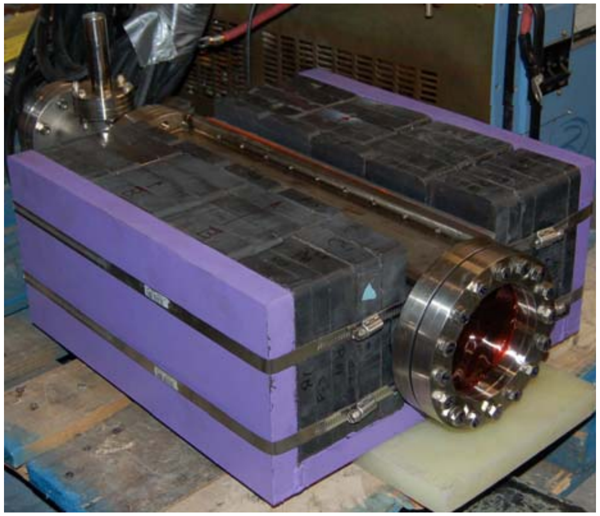

Deuteron Photodisintegration Kinematics

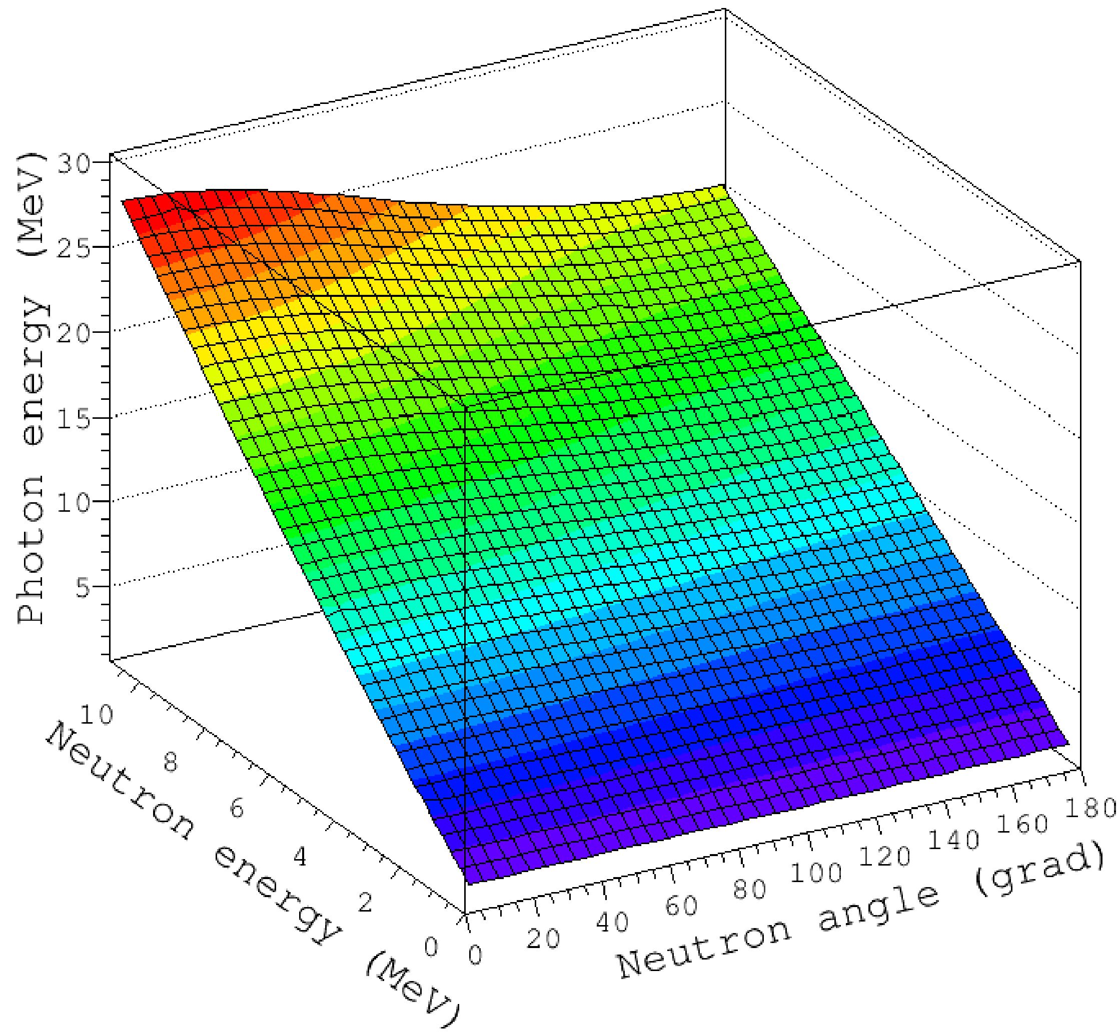

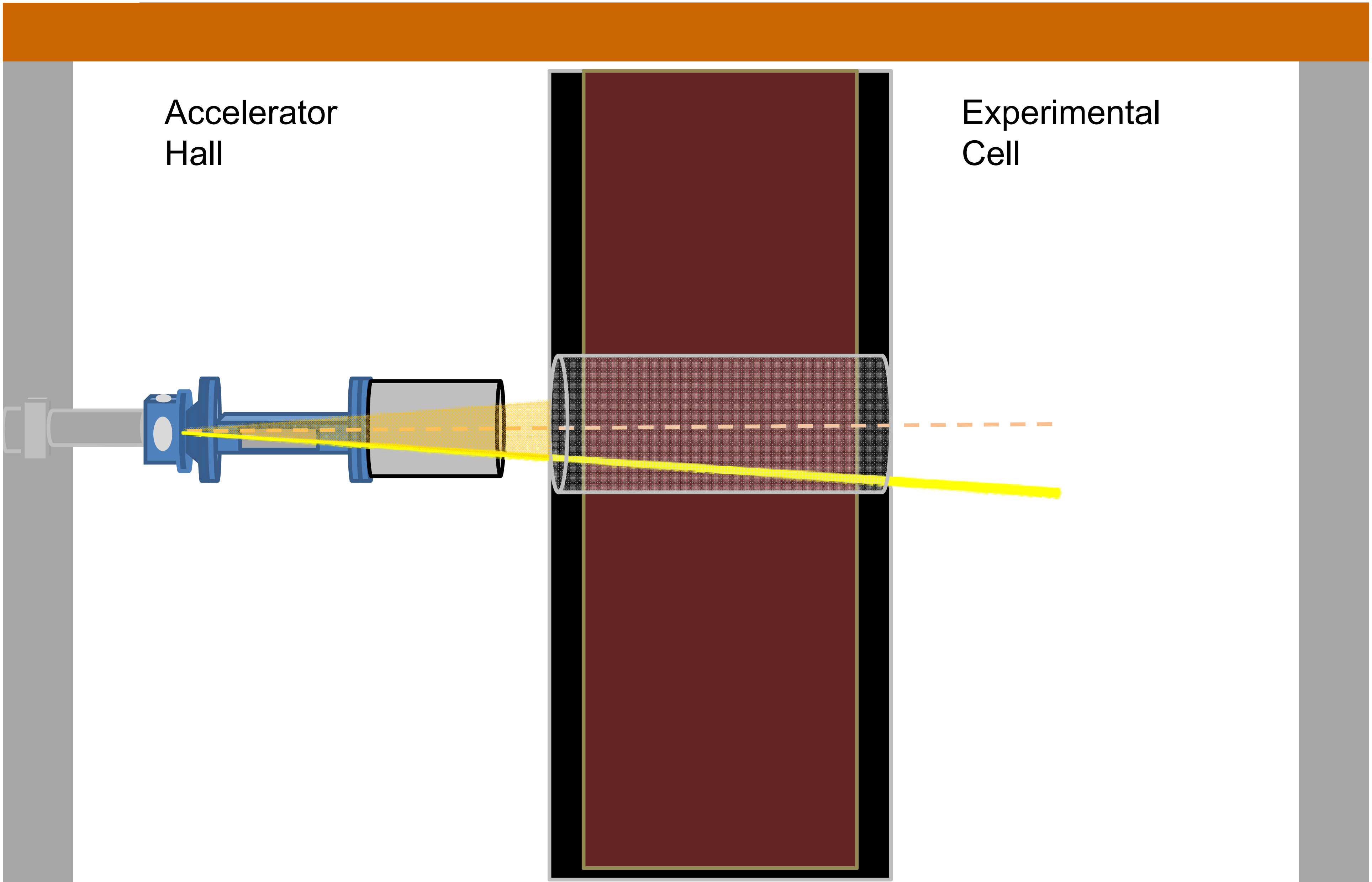

ISU PHYSICS

Idaho Accelerator Center

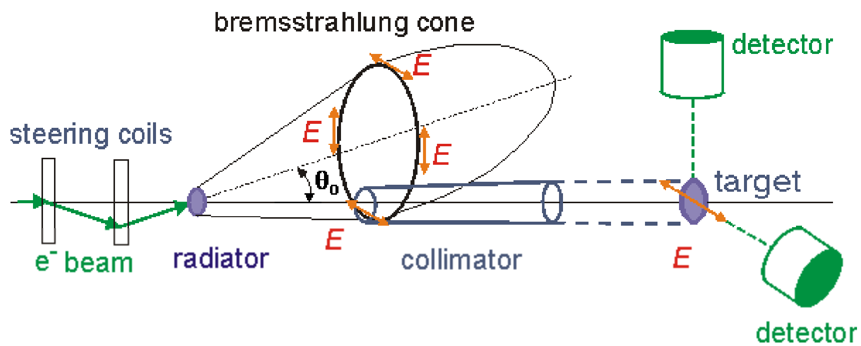
bremsstrahlung cone
detector
steering coils
E
E
E
E
θ_0
target
E
E
e⁻ beam
radiator
collimator
detector

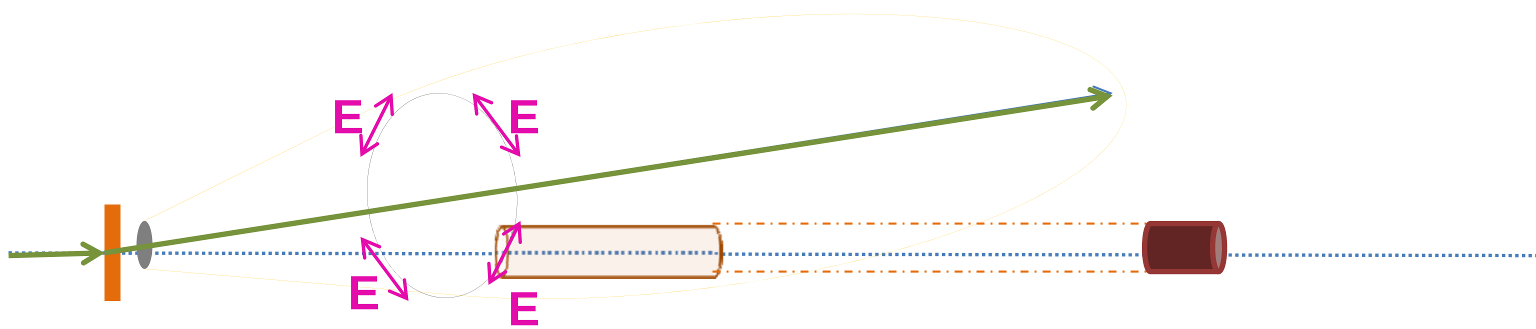
E
E
E
E

44 MeV Linac at Idaho Accelerator Center

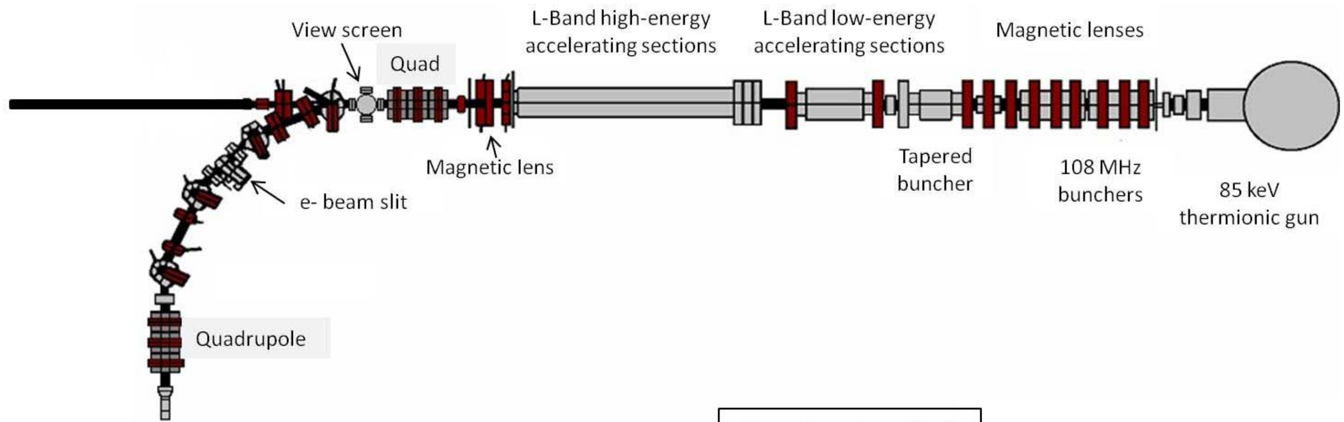

44-MeV Short Pulsed Linac
- 1.3 GHz L-band traveling-wave linac
- 2 ns pulse width
- 150 Hz rep rate
-1 nC/pulse (2 ns width)
- 25 MeV

Accelerator Hall

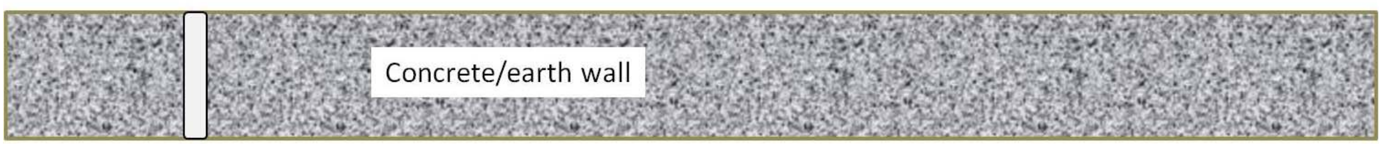

Experimental Cell

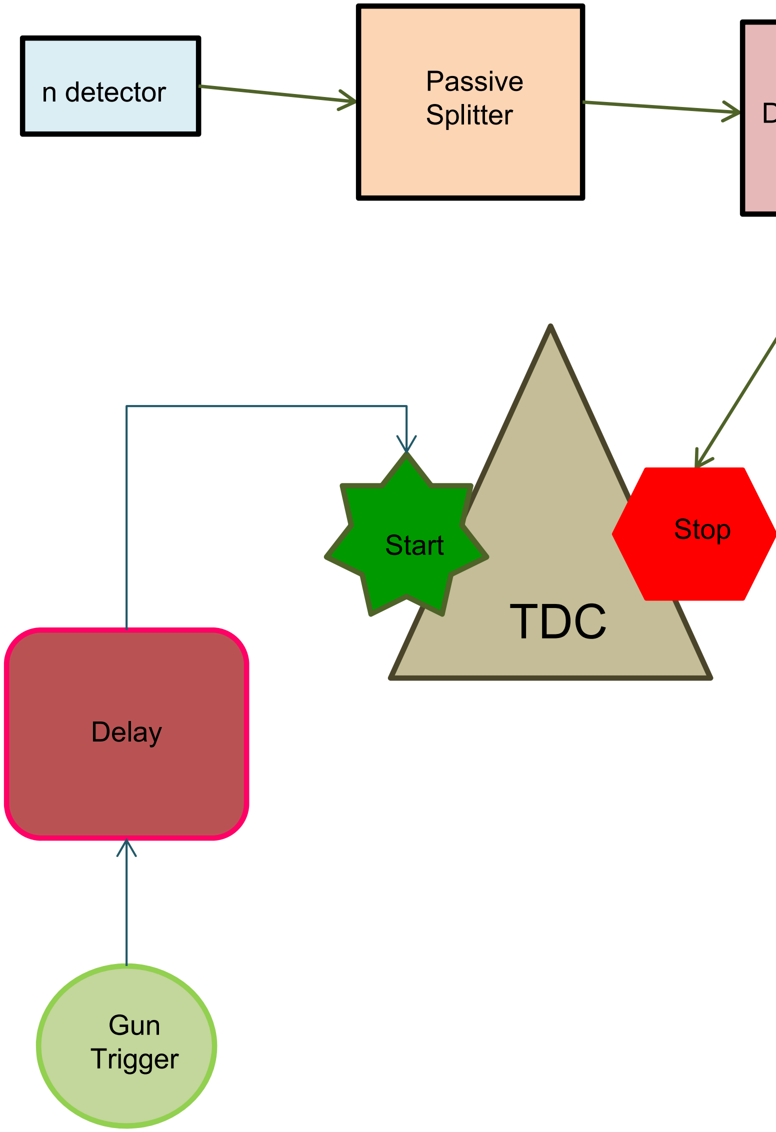

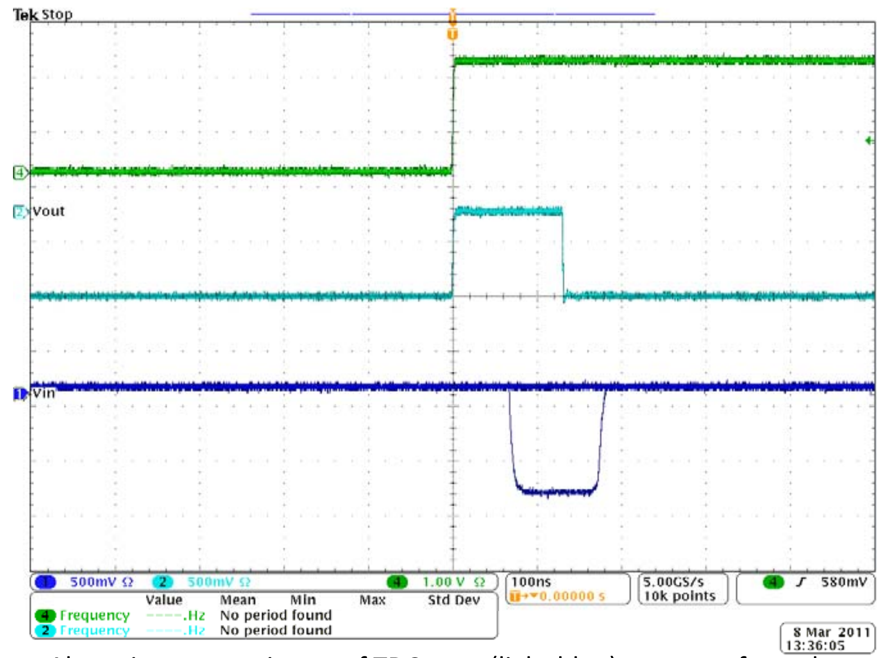

Above is a scope picture of TDC start (light blue), stop out from the discriminator (Ortec CF8000)(dark blue), and the gun pulse (green). The TDC is operated between the fall of the start and the rise of the stop (100ns).

H2O Background

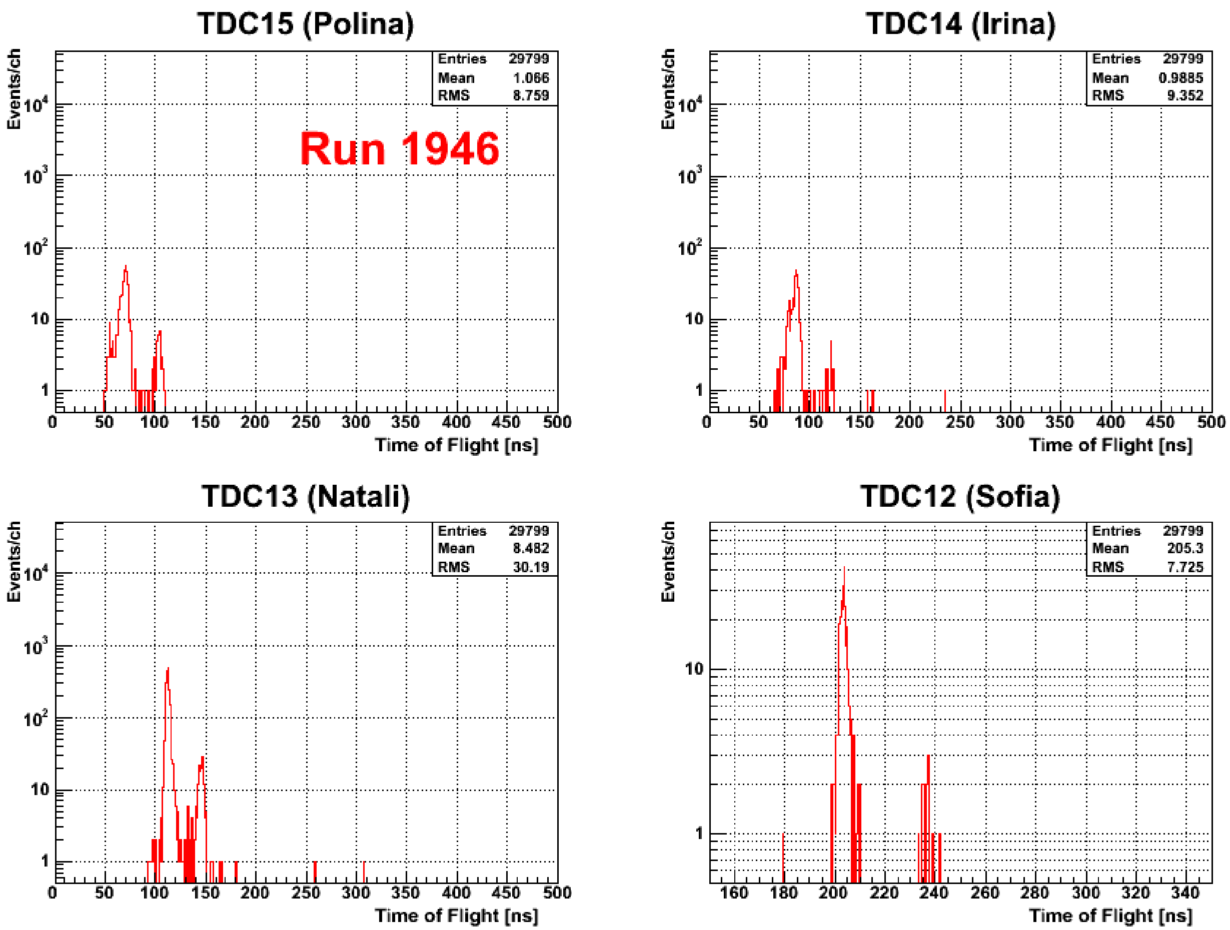

Liquid Drop Model

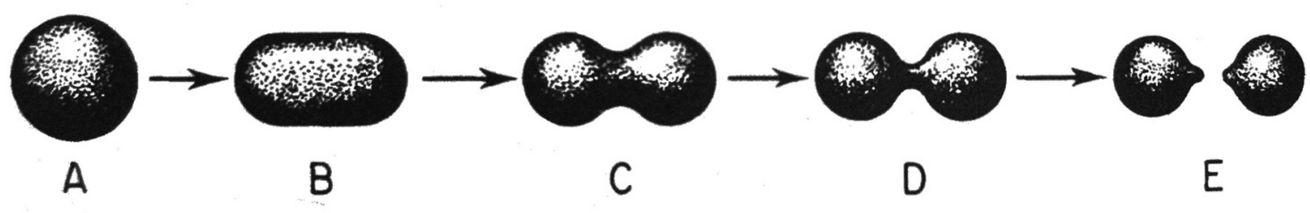

A. Energy of excitation suddenly added to the structure, as in absorption of gamma, will spread rapidly throughout the nuclear volume
B. The nucleus as a whole will be set into oscillation, changing from spherical configuration to an ellipsoid.
C. The electrostatic force of repulsion will tend to decrease, as some of the protons are now farther apart on the average than they were before.
    1. The surface to volume ratio has increased, reducing the effectiveness of the nuclear force resulting in a series of rapid oscillations
D. If the amplitude of the oscillation exceeds some critical value, a central constriction will appear. The nuclear force across this reduced area will no longer be able to hold together the two parts of the dumbbell-shaped nucleus.
E. The restriction narrows rapidly and pinches off, releasing the 2 fission fragments